minerals

MDPI

Article

Spatial Patterns and Source Apportionment of Potentially Toxic Elements in Flood-Affected Fluvisol Soils of the Bosna River Alluvial Plain

Elvir Babajić [1], Alisa Babajić [1], Samir Ustalić [2], Zoran Kovač [3], Tomislav Brenko [3], Marko Cvetković [3] and Stanko Ružičić [3,*]

[1] Faculty of Mining, Geology and Civil Enginnering, University of Tuzla, 75000 Tuzla, Bosnia and Herzegovina; elvir.babajic@untz.ba (E.B.); alisa.babajic@untz.ba (A.B.)
[2] Institute of Concrete Structures and Building Materials, Karlsruhe Institute of Technology, 76131 Karlsruhe, Germany; samir.ustalic@kit.edu
[3] Faculty of Mining, Geology and Petroleum Engineering, University of Zagreb, 10000 Zagreb, Croatia; zoran.kovac@rgn.unizg.hr (Z.K.); tomislav.brenko@rgn.unizg.hr (T.B.); marko.cvetkovic@rgn.unizg.hr (M.C.)
* Correspondence: stanko.ruzicic@rgn.unizg.hr

Abstract

This study quantifies the concentrations, spatial patterns, and sources of potentially toxic elements (PTEs) in Fluvisols from the Bosna River floodplain. Total As, Cr, Ni, Cu, Zn, Ba, V, and Co contents locally exceed national thresholds (e.g., As > 15 mg/kg, Cr > 80 mg/kg, Ni > 40 mg/kg), yet Ti-normalised enrichment factors mostly remain in the "no to minor" range (EF ≈ 1–3) and contamination factors in the "low to moderate" range (CF ≈ 1–3), indicating only slight to moderate enrichment even where absolute concentrations are high. Cr, Ni, Co, Ba, and V display similar spatial patterns, strong positive correlations with Mg and Fe, and consistently low EF values, confirming their predominantly geogenic origin linked to ultramafic and mafic parent rocks. In contrast, Cu, Zn, Pb, and Cd form coherent spatial clusters, share positive correlations, and show slightly elevated EF and CF values in flooded soils (typically EF and CF between 1 and 3), indicating diffuse industrial and agricultural inputs superimposed on a strong natural background. Flooding did not uniformly increase PTE concentrations but enhanced spatial heterogeneity and reorganised geochemical associations, particularly for Zn, As, and Cd, while the observed links between inorganic carbon (TIC), Ca, and Mg indicate that carbonate buffering and base cations help constrain metal mobility rather than exert a dominant control on all elements. The novelty of this work lies in integrating Ti-normalised EF and CF referenced to a local Fluvisol background with high-resolution GIS mapping and paired flooded versus control multivariate analysis, providing a quantitative, transferable framework to disentangle geogenic and anthropogenic signals and to prioritise post-flood monitoring of As, Cu, Zn, Pb, and Cd in naturally metal-rich floodplains.

Keywords: PTE; flood-affected soil; geochemical indices; spline; PCA; HCA

Academic Editor: Saglara S. Mandzhieva

Received: 26 March 2026
Revised: 11 May 2026
Accepted: 12 May 2026
Published: 14 May 2026

1. Introduction

Soil contamination by potentially toxic elements (PTEs) is recognised as a major environmental issue due to its long-term impacts on ecosystem functioning, food safety, and human health. Elevated concentrations of PTEs such as Cd, Pb, Ni, Cr, Zn, and Cu in soils are frequently reported in industrialised and urbanised regions, where both natural

(geogenic) and human-related (anthropogenic) processes contribute to their accumulation. Differentiating between these sources is essential for designing appropriate monitoring strategies, conducting risk assessments, setting regulatory thresholds, implementing land-use management interventions, and prioritising remediation measures.

Fluvisols developed on river alluvial plains are particularly vulnerable to contamination by PTEs because they receive inputs from upstream geological formations as well as from point and diffuse pollution sources transported by water and sediments. Vácha et al. [1] showed that Fluvisols in the Labe fluvial zone have increased geogenic loads (e.g., Be, As) and elevated, more extractable contents of other trace elements indicative of anthropogenic inputs. Martynov [2] found that Fluvisols in the Amur River valley can be heavily contaminated when element contents in the catchment area are high due to both geogenic and anthropogenic sources, with subsequent downstream redistribution during floods, while Ružičić et al. [3] confirmed similar in the Sava River valley. Forstner et al. [4] and Lair et al. [5] discussed contamination of Fluvisols in floodplains by upstream industrial and mining activities. Krami et al. [6] found that Cd, As, and Cu are associated with the discharge of industrial wastes, the exploitation of mines for special mineral ores, and fertilisers from agriculture.

In Bosnia and Herzegovina and the wider Western Balkan region, increased concentrations of Ni, Cr, Cd, As, and other metals in soils and sediments have been linked to industrial facilities, and coal-fired power plants and associated ash landfills, as well as historical pollution and inadequate waste management [7]. The Bosna River, which drains several urban and industrial centres, has been identified as a recipient of municipal and industrial wastewaters, raising concerns about the quality of its water and the adjacent soils and sediments [8,9]. In the study area, environmental problems with metals near the Bosna River include the input of toxic heavy metals (notably As, Pb, and Cd) into the soils due to industrial and urban wastewater, mining, and associated land use.

To obtain information about potential sources of PTEs in Fluvisols developed on the Bosna River plain, geochemical indices such as the enrichment factor (EF) and contamination factor (CF) were used. The enrichment factor (EF) quantifies the increase in the concentration of an element in soil relative to a reference baseline and helps distinguish natural from anthropogenic inputs of that element [10].

According to [10], the enrichment factor (EF) is strongly influenced by the choice of background or baseline values, which can vary significantly with local geology and spatial scale, as well as by the selection of a 'conservative' reference element that may, in practice, be affected by the same processes as the metals of interest. In addition, the contamination factor (CF) is also based on ratios to background concentrations, showing a strong dependence on how background or baseline values are defined and the inability of simple concentration-based indices to fully distinguish natural from anthropogenic contributions.

It has been shown that various statistical analyses can be used to evaluate relationships between different soil properties, ranging from correlation analysis [11,12] to multivariate analyses such as cluster analysis [13–15] and principal component analysis (PCA; [16–18]). Some research has shown that cluster analysis and PCA are widely used statistical methods when only a limited data set is available [15,19]. However, it has also been found that PCA can sometimes have difficulty identifying differences in soil quality with respect to different management systems [20].

Examining the distribution and sources of PTEs in soil is crucial for controlling soil pollution, reducing health risks, and achieving sustainable land use [21]. Therefore, the spatial distribution of PTEs was modelled using GIS-based mapping in our study. Monaci and Baroni [22] investigated the spatial distribution of PTEs and found that contamination exhibits clear spatial patterns influenced by local topography and historical land use. This

approach integrates spatial interpolation with multivariate statistical analyses (correlation matrices, cluster analysis, and principal component analysis) to link spatial variation with possible geogenic and anthropogenic sources. This combined spatial–statistical methodology enhances understanding of PTE behaviour across the landscape and provides a replicable tool for environmental assessment.

However, most of these studies have focused on upstream contamination zones, offering limited insight into how combined geogenic and anthropogenic factors interact within downstream floodplain environments. This lack of integrated source discrimination in floodplain Fluvisols creates uncertainty in understanding the relative contributions of natural background and human-induced enrichment.

Addressing this gap, the present study focuses specifically on Fluvisols developed in flood-affected river basins, aiming to disentangle overlapping geogenic and anthropogenic signals through a combination of geochemical, statistical, and spatial approaches. In doing so, it seeks to clarify source–process relationships governing PTE accumulation in floodplain soils and to improve the reliability of contamination assessment in these hydrologically dynamic environments.

To our knowledge, this is the first study to investigate PTEs in Fluvisols of the Bosna River alluvial plain using paired flooded and non-flooded Fluvisols within a single, well-constrained ultramafic catchment, rather than relying solely on regional or literature backgrounds. Additionally, this work advances previous Fluvisol case studies [1–4,7] by jointly applying Ti-normalised EF/CF, statistical analysis, and high-resolution GIS mapping to distinguish geogenic from anthropogenic PTE patterns in a post-flood setting.

The main objectives of this research were to: (1) determine the spatial patterns of PTEs in Fluvisol soils after the Bosna River flood; (2) identify their natural or anthropogenic sources by integrating statistical methods and GIS; (3) assess the level of PTE contamination in flooded soil based on geochemical indices; and (4) explore the possible influence of flooding on the spatial distribution and PTE contamination.

2. Materials and Methods

2.1. Study Area Description

The study area of Maglaj municipality is located in the north-eastern part of Bosnia and Herzegovina (Figure 1A), covering approximately 289 km^2, which includes the town of Maglaj and its surroundings. The relief of the wider Maglaj area is characterised by river valleys and terraces, low slopes, and hills. The morphometric breakdown is moderate, with an average hypsometric range from 170 m (Bosna river valley) to 530 m (north-west of Parnica). The area is characterised by a moderate continental climate (Cfwbx in the Köppen climate classification system) with four distinct seasons.

The lithostratigraphic characteristics of the wider Maglaj area are presented on the geological map (Figure 1B), based on data from the basic geological map of the Zavidovići sheet [23] and supplemented by new research [24].

Peridotites, represented mainly by lherzolites and their alteration products, serpentinites, are the oldest and most widespread rocks in the wider Maglaj area. Their contact with the surrounding sediments is clearly tectonic [23].

Gabbroperidotites, mafic microgabbros, and dolerites most often occur in contact areas between ultramafic masses and sediments of the ophiolite mélange. Spilites usually lie concordantly within the sediments and represent products of submarine outpouring that occurred simultaneously with the deposition of "younger" Jurassic sediments. The ophiolite mélange (J2,3) represents a chaotic lithological unit where rocks belonging to ophiolites also appear in the tectonised matrix composed of Pelasgian and abyssal sediments, greywackes, cherts, and clays.

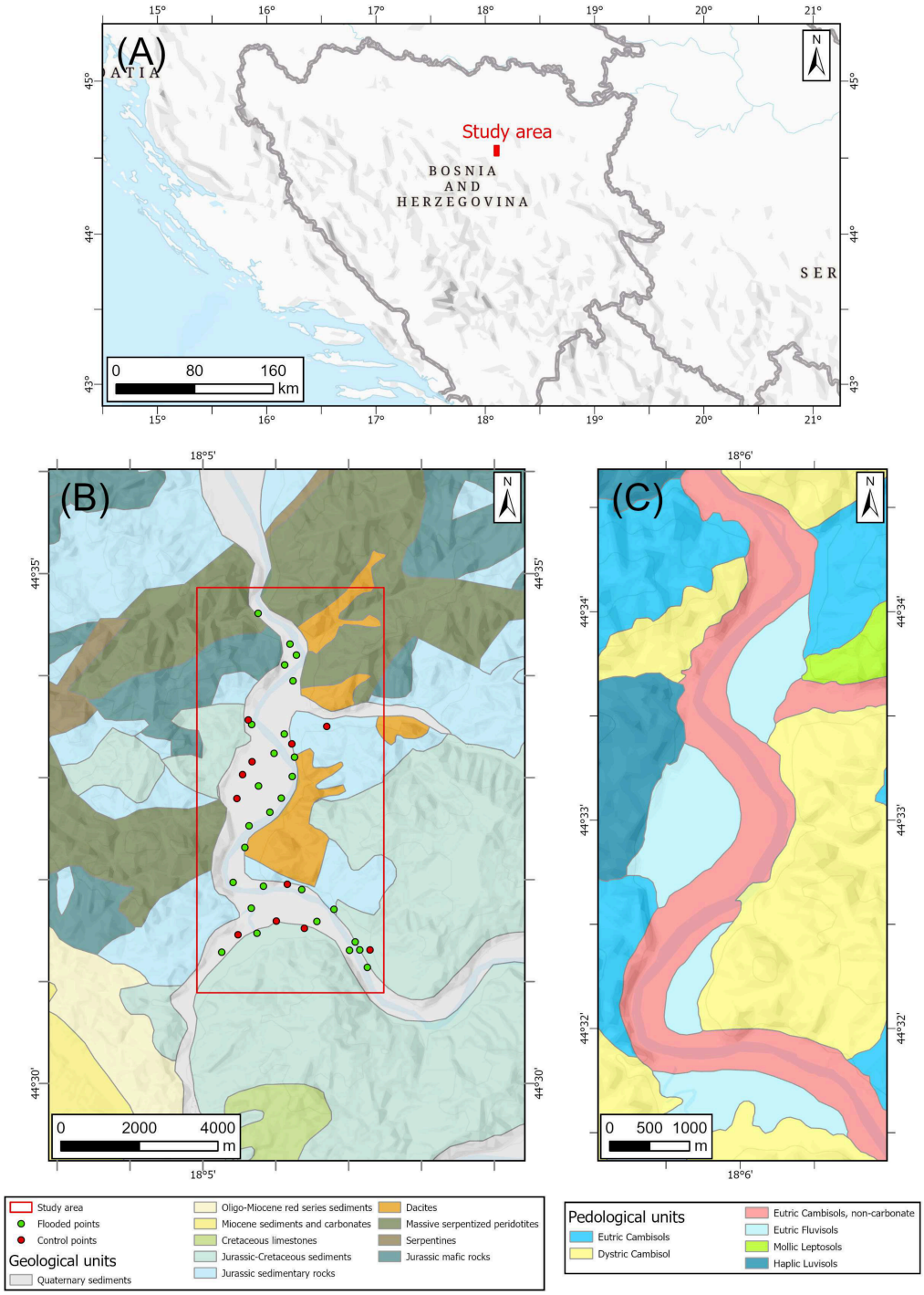

Figure 1. (**A**) Location of study site within north-central Bosnian region; (**B**) geological map of the study area with sampling sites of control and flooded samples; and (**C**) pedological map of the study area according to [23,25].

Formations of Jurassic–Cretaceous age (J, K) are represented by a thick sequence of clastites lying transgressively over the ophiolitic mélange formations. Several masses of dacitic (aqM) rocks are products of Neogene volcanism.

Quaternary deposits (Q) in the Bosna River valley and its tributaries consist of unconsolidated to weakly consolidated fluvial sediments, which lithologically belong to clastic sediments. Gravels, sands, silts, and clays predominate, occurring in various granulometric associations and mutual relationships.

The gravels are typically polymict and poorly sorted, composed of rounded to sub-rounded clasts of diverse petrographic composition, with a predominance of lithoclasts of igneous rocks. The sands are medium to poorly sorted, predominantly of quartz–feldspar composition, while the fine-grained fractions are represented by silts and clays, with local occurrences of organic matter. In the vertical profile of the Quaternary deposits, lithofacies members are clearly differentiated: basal gravels with coarse-clastic texture and high permeability, overlain by sand layers with well-developed cross-bedding, and capped by horizons of silts and clays that exhibit laminated to massive texture and low permeability. This sequence reflects a typical sedimentary succession characteristic of fluvial systems. Pronounced lateral and vertical facies changes are manifested through the alternation of coarse-clastic and fine-clastic sediments, indicating variable hydrodynamic conditions during deposition. Such heterogeneity results from a multi-phase development of the river system, including periods of intense erosion, transport, and redeposition of material during high-water events.

Quaternary deposits therefore represent not only a record of fluvial dynamics, but also an active geochemical medium in which the distribution and concentration of potentially toxic elements (PTEs) occur.

District Cambisol dominates the territory of the municipality of Maglaj (Figure 1C). Significant areas are covered by Eutric Cambisol, followed by Luvisol. Humofluvisols are soils found in river valleys; they are young soils with a developed A horizon formed on alluvial sediments. In the Maglaj area, both automorphic and hydromorphic soils have developed [25]. According to the international classification (FAO, 2015), Eutric Fluvisol is defined as a reddish-brown, carbonate-free soil (symbol—Fle), and in the national classification it is called humofluvisol. Eutric non-carbonate Fluvisol (symbol—Fle) belongs to the group of alluvial non-carbonate soils, i.e., Fluvisols according to the national classification.

2.2. Field and Laboratory Work

Field research was conducted in autumn 2016 over an area of approximately 5 km^2, approximately two years after the flood occurred. As shown in Figure 1C, sampling was conducted in the plain area affected by the 2014 floods. All 45 samples were taken from two types of soil (Figure 1B): Eutric Fluvisol (EF)—34 samples (flooded; 75%)—and non-carbonate Eutric Fluvisol (Efnc)—11 samples (control; 25%). Samples were taken in a square formation (one central and four marginal samples) with a distance of 2 m between points. The sampling network was established based on analysis of the area affected by the flood, accessibility of micro-localities, and the geological and pedological composition of the terrain. Control samples were taken from the unflooded part of the study area, without anthropogenic influence.

Soil samples were collected at each sampling site using a small plastic shovel from five shallow pits. The sampling depth was 10–25 cm, with 10 cm of humus surface litter and plant residues removed. Subsamples were collected within a 2 × 2 m square, consisting of one central and four marginal points. One composite sample was prepared for each sampling site, each containing about 2 kg of soil. Soil samples were air-dried and passed through a 2 mm sieve for laboratory analysis.

Total concentrations of elements, i.e., Mo, Cu, Pb, Zn, Ni, Co, Mn, Fe, As, Cd, V, Cr, Ba, Zr, Li, Al, Ca, Mg, Na and K, were analysed by Inductively Coupled Plasma Mass Spectrometry (ICP-MS) after complete dissolution of samples using aqua regia solution. Instrumental precision, determined through five measurements alongside blanks and standards, maintained a margin of error of ±5% or less. The accuracy of the analyses was further controlled using certified geological reference materials (DST5, ACME Laboratory; n = 5, Appendix A.1).

Soil particle size distribution (clay < 2 μm, silt 2–63 μm, sand 63–2000 μm, gravel > 2000 μm) was determined by the pipette method with sieving and sedimentation after dispersion with sodium pyrophosphate, and interpreted according to FAO (2006). Soil pH was measured in water at a 1:5 soil to water ratio (ISO 13536:2005) using a Multi 340i WTW pH meter (WTW GmbH, Weilheim, Germany) (Appendix A.2).

Total carbon (TC), total inorganic carbon (TIC), and total sulphur (TS) analyses were performed on soil samples to calculate the percentage of organic matter. The analyses were conducted using the Multi EA 4000 CS analyser (Analytik Jena GmbH+Co. KG, Jena, Germany) by the dry combustion method for TC and TS, while the TIC value was obtained by dissolving the carbonates with 30% H_3PO_4 acid in the manual TIC module of the EA 4000 CS analyser. For all analyses, approximately 600 to 800 mg of previously dried, crushed, and ground samples were used. The total organic carbon (TOC) value was calculated by subtracting the TIC from the TC value (Appendix A.2).

2.3. Geochemical Indices

The EF is calculated and presented in Appendix A.3 as the ratio of the studied element to the reference element, normalised by the same ratio for the composition of the continental crust [26]. Titanium (Ti) has been used as reference element because it is considered geochemically stable, hosted by resistant minerals, and conservative in most geochemical environments. It is an abundant metal, and its concentrations are unlikely to be significantly affected by anthropogenic sources [27]. Several authors have used Ti to normalise heavy metals [28,29].

The formula to calculate EFs can be generalised as follows (where "crust" can be replaced by a local background):

$$EF_{El} = (El_{sample}/X_{sample})/(El_{crust}/Xc_{rust}), \quad (1)$$

where El_{sample}/X_{sample} represents the ratio of the concentration of the analysed element (El_{sample}) to the concentration of Ti (X_{sample}), while El_{crust}/X_{crust} is the ratio of the concentrations of elements (Ba, Cu, Co, Mo, Li, Zn, As, V, Cr, Ni, Cd, Pb) in local background materials to the background concentration of Ti in local materials, i.e., the median values of metal concentrations in control soil samples. According to [30], EF < 1 indicates no enrichment; 1–3, minor enrichment; 3–5, moderate enrichment; 5–10, moderately severe enrichment; 10–25, severe enrichment; 25–50, very severe enrichment; and >50, extremely severe enrichment.

The contamination factor (CF, Appendix A.4) is defined as the ratio between the measured concentration of the PTEs in the samples and the background level of the corresponding PTEs [31]. The contamination factor is classified into four groups by [32]: low ($CF < 1$), moderate ($1 \leq CF \leq 3$), considerable ($3 \leq CF \leq 6$), and very high ($CF > 6$).

2.4. Statistical Analysis

Main statistical parameters (average, standard deviation, and coefficient of variation—Cv) were calculated for all observed parameters for both flooded and control samples, totalling 28 parameters. Correlation, cluster, and factor analyses were performed using TIBCO Statistica (version 14.0.0.15), while all data was standardised to z-values due to the different units of the inspected variables. Correlation matrices are presented in the Appendices A.5 and A.6. All statistically significant results are marked in red ($\alpha = 0.05$). Cluster analysis was performed using Ward's method and Euclidean distances, and a plot of linkage distances was used to define the number of clusters. The application of Ward's method has been found to be very useful in different types of soil research [33,34]. Principal components (PCs) were extracted using factor analysis in TIBCO Statistica. The

maximum number of factors was limited to the number of identified clusters to allow for a more representative comparison and data interpretation. Additionally, only factors with eigenvalues greater than 1 were retained, and the goal was to explain at least 70% of the total variance. Factor loadings higher than 0.7 are marked in red. For factor data interpretation, varimax raw rotation was used. Varimax rotation has previously been successfully applied in various types of soil research [35–37]. In general, correlation analysis was used to gain an initial insight into the relationships among the investigated variables. Due to the wide range of obtained values, multivariate statistical analyses were used for more detailed data interpretation. First, cluster analysis was used to identify the preliminary number of groups of associated variables. Then, together with the previously defined statistical criteria, the maximum number of clusters was used as the criterion for defining the maximum number of factors. In this way, results from both methods were evaluated and compared. Although cluster analysis provided information about preliminary grouping, factor analysis indicated which factors were more significant and which interpretations should be emphasised. It must be clearly stated that one of the main statistical limitations of this research is related to the imbalance between the number of flooded (n = 34) and control (n = 11) samples. Although soil research often compares different types of soil data [38–41] usage of different numbers of samples can be the consequence of different research scope, analytical focus, sampling methodology, etc. In general, when using different number of cases to compare two datasets it is always necessary to have in mind that it can influence results by affecting statistical significance, introducing bias, as well as generating lower accuracy and higher uncertainty. On the other side, similar numbers of samples in datasets can produce more reliable and robust results.

2.5. Spatial Distribution Analyses

The spatial distribution of selected PTEs was determined using the spline with barriers interpolation method, available within the Spatial Analyst Tools in ArcGIS Pro 3.0. Spline interpolation is widely used in soil geochemistry for estimating soil properties, as it produces smooth, continuous surfaces that effectively represent spatial variability [42]. The spline with barriers approach extends this method by accounting for abrupt changes in soil chemical properties, such as those caused by rivers or edge effects in contaminated areas, resulting in a more realistic representation of geochemical distribution. In this case, the Spline interpolation method was used instead of Kriging because the sampling grid for both flooded and control samples was highly irregular due to the terrain configuration. Although the spline interpolation method has extrapolation constraints, especially when predicting anomalies outside the sampling perimeter, it was estimated that these constraints are limited by using barriers (Bosna river alluvium).

For each element, a total of six maps was created: bulk geochemistry for flooded and control points, alongside the EF and CF for flooded and control data. Geochemical data were mostly classified into four or five classes, based on the range of geochemical quantities for each element, either using natural breaks (Jenks) classification methods or based on maximum allowable concentrations for each element. Classification for the EF and CF followed the methods described in [30,32].

3. Results and Discussion

3.1. Spatial Distribution of PTEs and Geochemical Factors

The physico-chemical characteristics of the analysed Fluvisols are presented in Appendix A.2. Across all samples, pH values are neutral to slightly acidic, ranging from about 6.8 to 7.5 in both flooded and control soils, with very similar means around 7.1–7.2. Particle size distributions indicate sand-dominated textures, with sand contents roughly

70%–90%, silt about 3%–20%, and gravel from 0% to 22%. Total carbon (TC) ranges from about 1.7% to 5.5%, with average TC values of approximately 2.72% (flooded) and 2.71% (control). Inorganic carbon (TIC) varies from near 0 up to about 2.2%, with averages of 0.47% (flooded) and 0.14% (control), and TOC, calculated as TC–TIC, ranges from roughly 0.8% to 4.0%, with averages of 2.25% in flooded and 2.57% in control soils.

The spatial distribution of PTEs and geochemical factors in the analysed soils is shown in Appendices A.1, A.3 and A.4. Several elements (As, Cu, Ba, V, Cr, Ni, Zn, Co) exceed the soil threshold values defined by the Official Gazette of the Federation of Bosnia and Herzegovina [43]. Arsenic levels (Figure 2a) show a variable distribution in the study area. Several zones with increased values, above 15 mg/kg [43], can be identified, particularly in the northern part of the flooded site. Figure 2b shows that As is predominantly distributed in the southern and southeastern parts of the control study area.

Arsenic concentrations exceeding threshold values in the Fluvisol soils of this study indicate levels elevated above typical background values reported for many alluvial soils. Natural As contents in uncontaminated soils are commonly around 5 mg/kg [44], so the concentrations determined in this study are generally considered indicative of enrichment or contamination rather than purely geogenic background. Elevated As associated with floodplain and fluvial processes has been documented in several regions, where repeated flooding, sediment deposition, and upstream mining or industrial activities lead to accumulation of As in near-surface soils. In addition, the use of agrochemicals such as herbicides, insecticides, and fungicides can contribute to elevated concentrations of As in soils [45].

According to [30], the enrichment factor (EF) is classified as minor across almost the entire flooded study area (Figure 2c), whereas the control area shows a different distribution (Figure 2d). The northern part of the control study area is classified as showing no enrichment, while the southern part shows minor enrichment (Figure 2d). The enrichment pattern of As in the Fluvisols of the flooded study area suggests only limited anthropogenic impact. Such minor enrichment implies that natural geochemical processes, including parent material composition and flood-driven sediment deposition, likely play a dominant role in controlling As levels, rather than intensive local pollution. Consequently, the observed EF distribution supports the interpretation that the flooded Fluvisols are only slightly affected by As enrichment and currently remain within a low-risk contamination category. The contamination factor (CF) was mostly consistent with the EF, indicating that soils in the flooded study area are low to moderately contaminated with arsenic (Figure 2e). In the control area, the distribution is similar to that of the EF, and the classification is comparable to the flooded area (Figure 2f).

The EF results in this study indicate that arsenic enrichment is generally minor relative to the local geogenic background, implying limited additional anthropogenic input; however, this does not preclude environmental concern because absolute As concentrations frequently exceed regulatory thresholds for soils. Elevated As concentrations suggest that As in the study area should be treated as a parameter requiring targeted monitoring and site-specific risk assessment.

The Cu and Zn levels showed extremely high concentrations (65 mg/kg for Cu, 150 mg/kg for Zn) according to [43], particularly in the western part of the flooded site (Figures 3a and 4a).

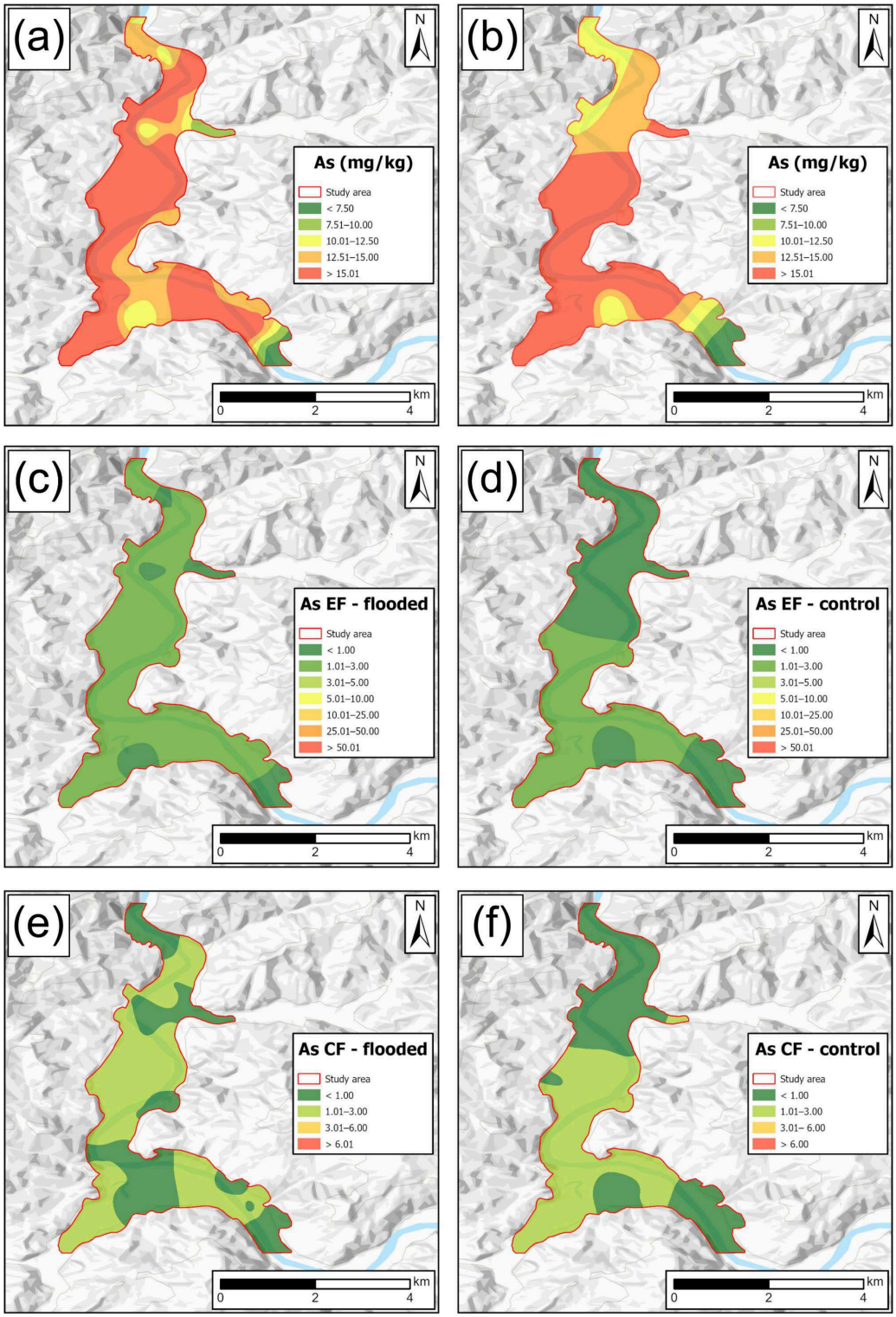

Figure 2. (**a**) Spatial distribution of As in flooded area; (**b**) spatial distribution of As in control area; (**c**) enriched factor for As in flooded area; (**d**) enriched factor for As in control area; (**e**) contamination factor for As in flooded area; (**f**) contamination factor for As in control area.

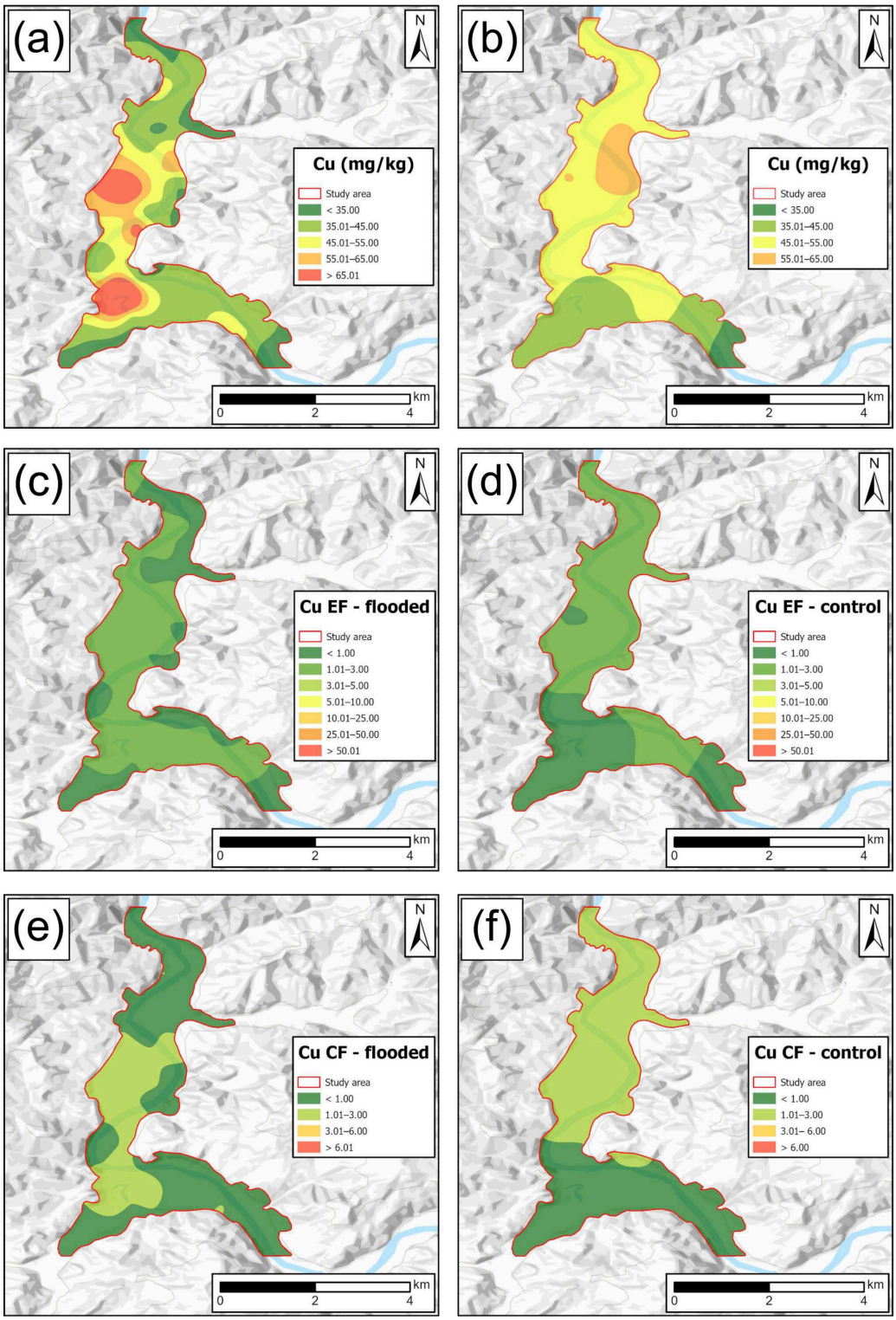

Figure 3. (**a**) Spatial distribution of Cu in flooded area; (**b**) spatial distribution of Cu in control area; (**c**) enriched factor for Cu in flooded area; (**d**) enriched factor for Cu in control area; (**e**) contamination factor for Cu in flooded area; (**f**) contamination factor for Cu in control area.

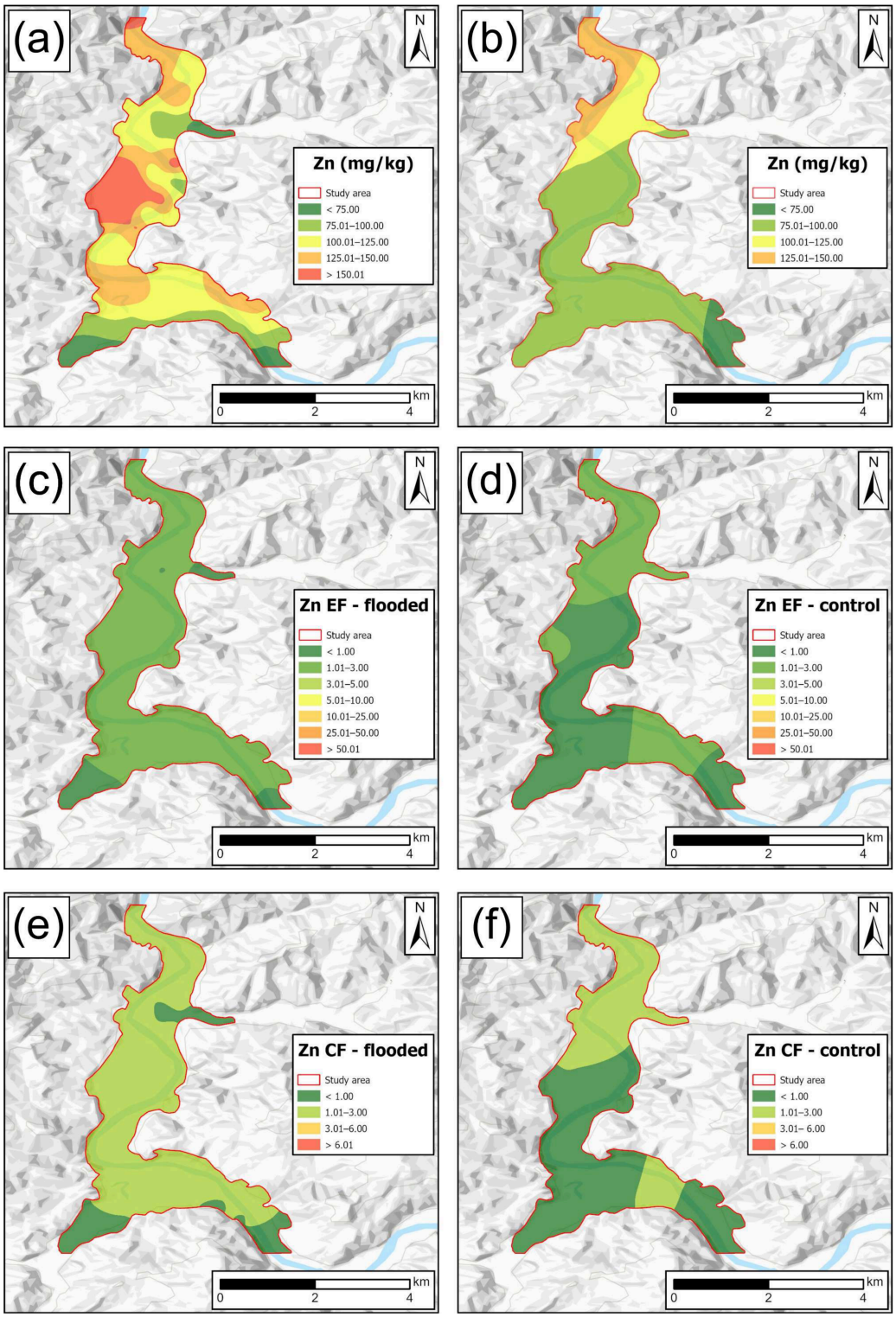

Figure 4. (**a**) Spatial distribution of Zn in flooded area; (**b**) spatial distribution of Zn in control area; (**c**) enriched factor for Zn in flooded area; (**d**) enriched factor for Zn in control area; (**e**) contamination factor for Zn in flooded area; (**f**) contamination factor for Zn in control area.

Figure 3b shows that Cu is predominantly distributed in the eastern part of the control area. This distribution differs from that of As and may therefore indicate a different source. Increased concentrations of Cu and Zn after the flooding event of the Bosna River were reported by [46]. The authors indicated that potential sources of Cu and Zn include industrial activities, such as the cellulose and paper factory in the Maglaj area.

The enrichment factor (EF) is classified as minor across almost the entire flooded study area (Figures 3c and 4c), while the control area shows a different distribution (Figures 3d and 4d). The northern part of the control area is classified as minor enrichment, whereas the south-west part shows no enrichment (Figures 3d and 4d). If the EF value reaches 2, soil contamination is caused by human activities or anthropogenic sources. In this study, the EF values for Cu and Zn ranged between 1 and 3, indicating that the concentration of PTEs in the soil may have been caused by natural processes rather than by anthropogenic activities. This is consistent with [2], who reported that, in many floodplain Fluvisols, Cu and Zn remain predominantly bound to clay minerals, Fe/Mn (hydr)oxides, and soil organic matter, which restricts their mobility and prevents strong surface accumulation even under alternating redox conditions during flooding.

Minor EF values for Cu and Zn do not exclude anthropogenic input, but rather indicate that such inputs are relatively low compared with the natural background signal. In many floodplain and Fluvisol settings, diffuse anthropogenic sources such as Cu- and Zn-based fungicides, manure, sewage sludge, and atmospheric deposition contribute additional Cu and Zn, but at levels that still fall into the low–minor EF classes. Minor EF values for Cu and Zn in the flooded Fluvisols therefore most likely reflect a combination of diffuse anthropogenic inputs (e.g., agriculture and atmospheric deposition) superimposed on a dominant geogenic background signal. This suggests that, although human activities contribute to Cu and Zn accumulation in the topsoil, their impact remains relatively low and does not lead to pronounced Cu and Zn enrichment across the flooded area.

The contamination factor (CF) was mostly consistent with the EF, indicating that soils in the flooded study area are low to moderately contaminated with PTEs (Figures 3e and 4e). In the control area, the distribution is similar to that of the EF, and the classification is comparable to the flooded area (Figures 3f and 4f). A similar study [47] in floodplain soils also reported low to moderate Cu and Zn contamination at sites influenced primarily by diffuse anthropogenic inputs rather than intensive point-source pollution.

The Cr and Ni levels showed extremely high concentrations (80 mg/kg for Cr, 40 mg/kg for Ni) according to [43] for both sites (Figures 5a,b and 6a,b). Both analysed PTEs exhibit an almost identical spatial distribution. These two elements predominantly originate from geogenic sources. According to [48], Cr and Ni are genetically related to the most frequent rock type in the wider area of Maglaj—ultramafic rocks.

The enrichment factors (EFs) for Cr and Ni are classified as minor across almost the entire flooded study area (Figures 5c and 6c), while the control area shows a different distribution (Figures 5d and 6d). The northern part of the control study area is classified as no enrichment, whereas the south-west part shows minor enrichment. This pattern is consistent with the ultramafic lithology of the terrain, where both Cr and Ni exhibit EF values slightly above 1. Low enrichment factors (EF < 3) for Cr and Ni have also been reported in Fluvisols of European floodplains and are attributed mainly to geogenic inputs from alluvial parent material rather than strong anthropogenic pollution [2,49,50].

The contamination factors (CFs) were mostly consistent with the EFs, indicating that soils in the flooded and control study areas are low to moderately contaminated with Cr and Ni (Figures 5e,f and 6e,f). Contamination factors for Ni and Cr typically fall within low to moderate contamination classes, with CF values commonly around 1–3 and only exceeding 6 in strongly industrial or mining-impacted Fluvisols such as those reported from Germany [51].

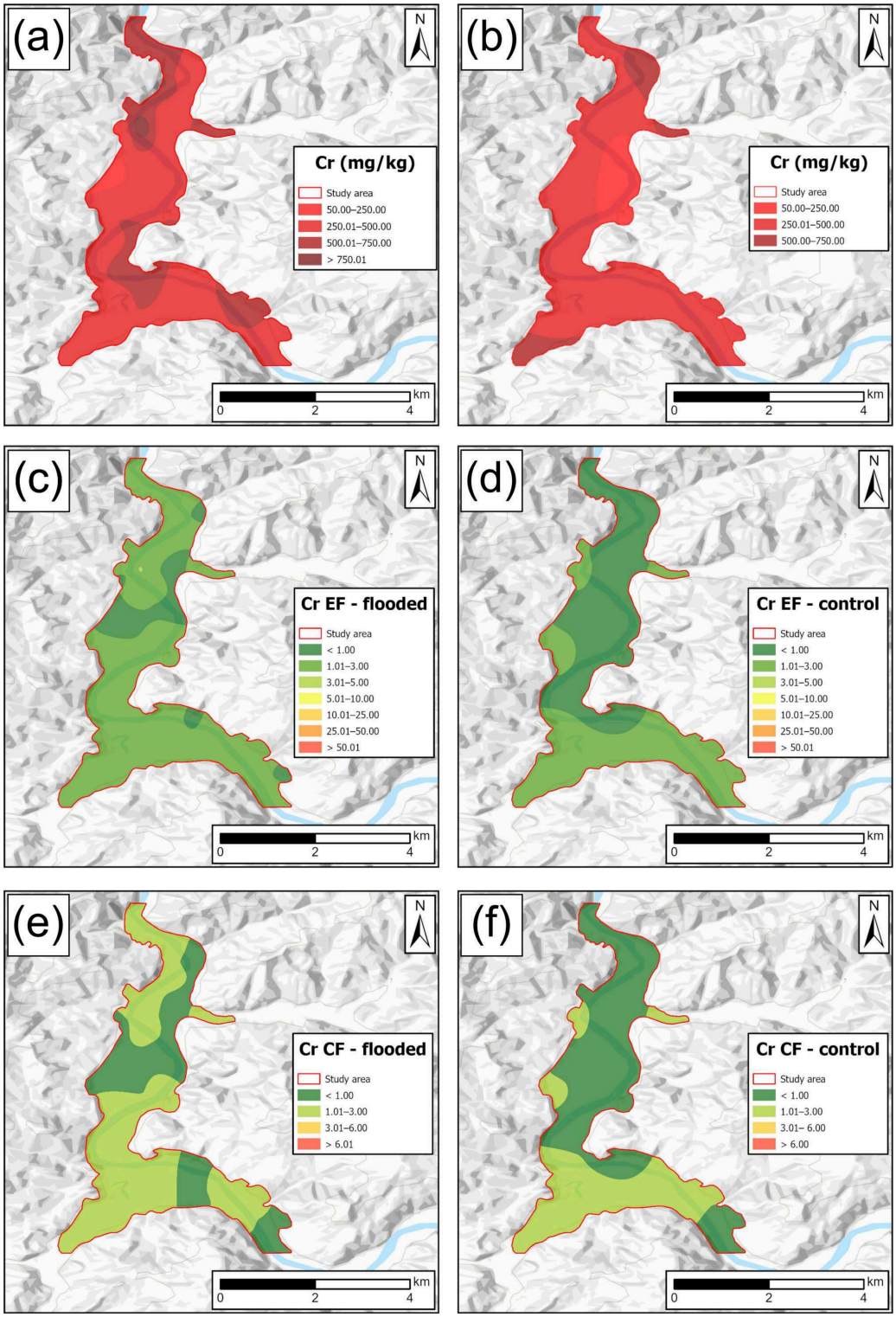

Figure 5. (**a**) Spatial distribution of Cr in flooded area; (**b**) spatial distribution of Cr in control area; (**c**) enriched factor for Cr in flooded area; (**d**) enriched factor for Cr in control area; (**e**) contamination factor for Cr in flooded area; (**f**) contamination factor for Cr in control area.

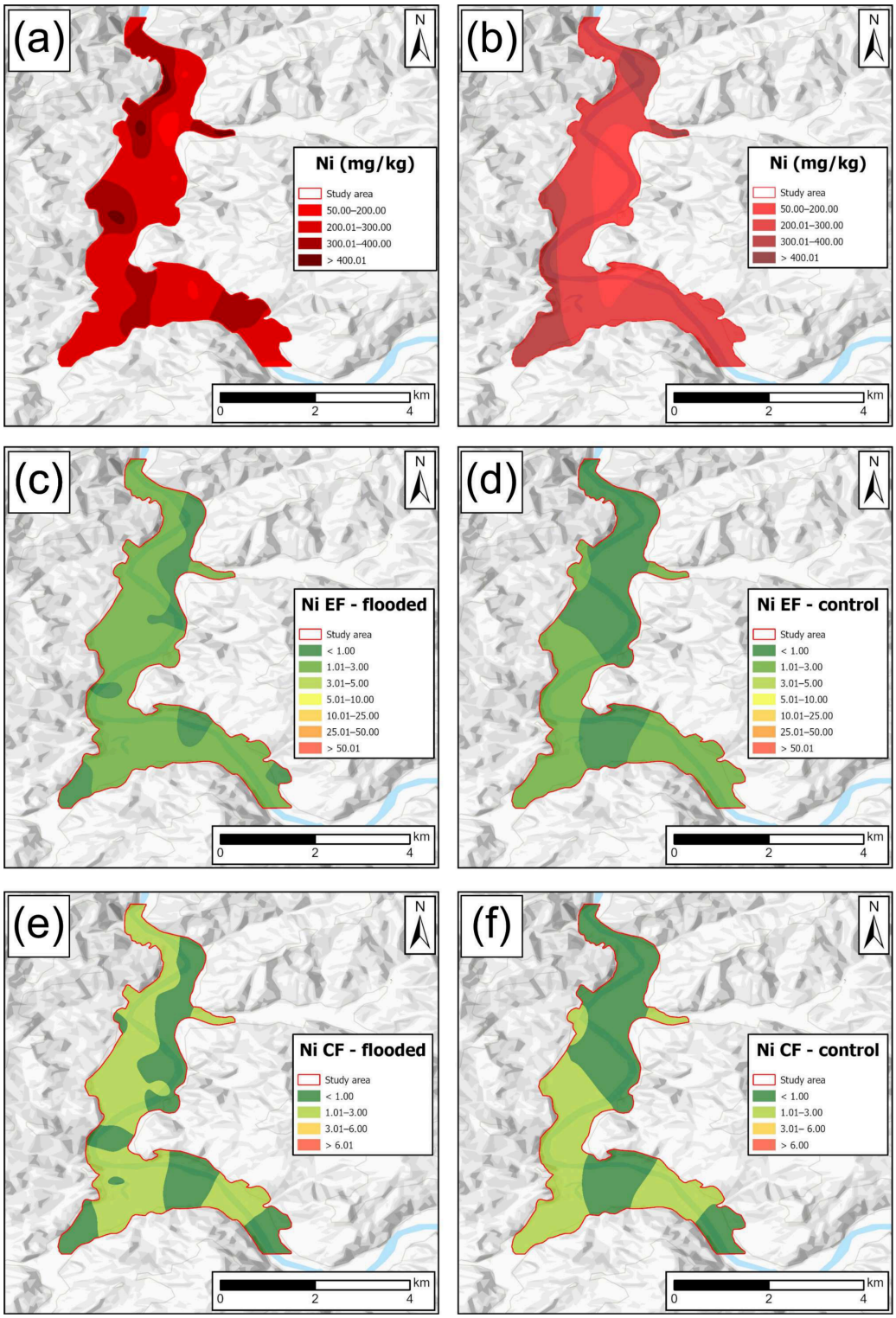

Figure 6. (**a**) Spatial distribution of Ni in flooded area; (**b**) spatial distribution of Ni in control area; (**c**) enriched factor for Ni in flooded area; (**d**) enriched factor for Ni in control area; (**e**) contamination factor for Ni in flooded area; (**f**) contamination factor for Ni in control area.

The Ba and V levels showed extremely high concentrations (80 mg/kg for Ba, 40 mg/kg for V) according to [43] at both sites (Figures 7a,b and 8a,b). According to [52], the behaviour of Ba depends on its association with potassium in rocks and its frequent occurrence in alkaline feldspars and biotites, which is consistent with our study area, underlain by igneous rocks, mainly dacites. In addition, V behaves similarly to Ba, as this

element also naturally occurs as a trace element in soils and sediments [53]. In our case, V distribution can be linked to mafic igneous rocks (dolerites and gabbroperidotites) and their geochemical characteristics. Therefore, the V concentrations can be related to the parent material, indicating a predominantly geogenic origin.

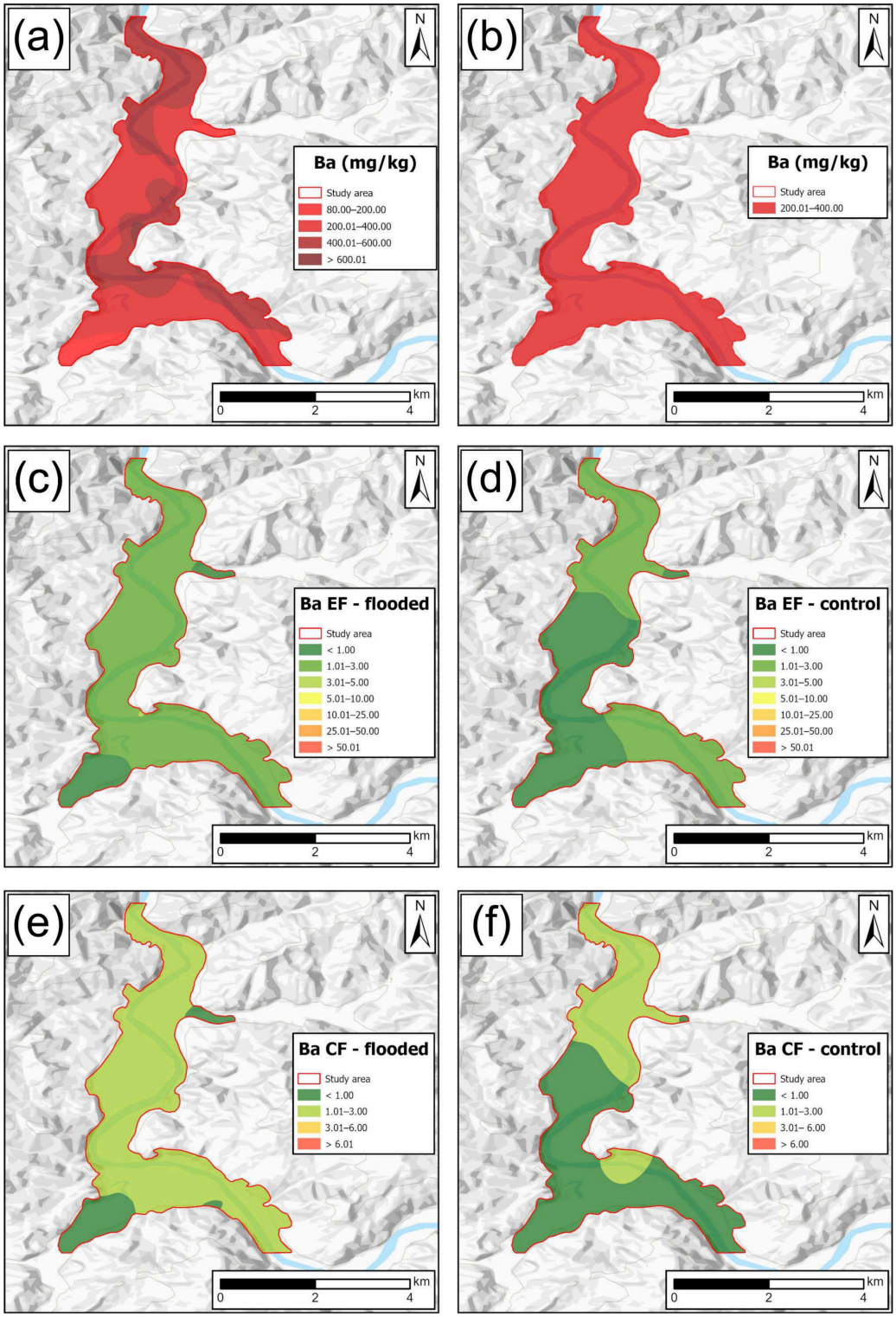

Figure 7. (**a**) Spatial distribution of Ba in flooded area; (**b**) spatial distribution of Ba in control area; (**c**) enriched factor for Ba in flooded area; (**d**) enriched factor for Ba in control area; (**e**) contamination factor for Ba in flooded area; (**f**) contamination factor for Ba in control area.

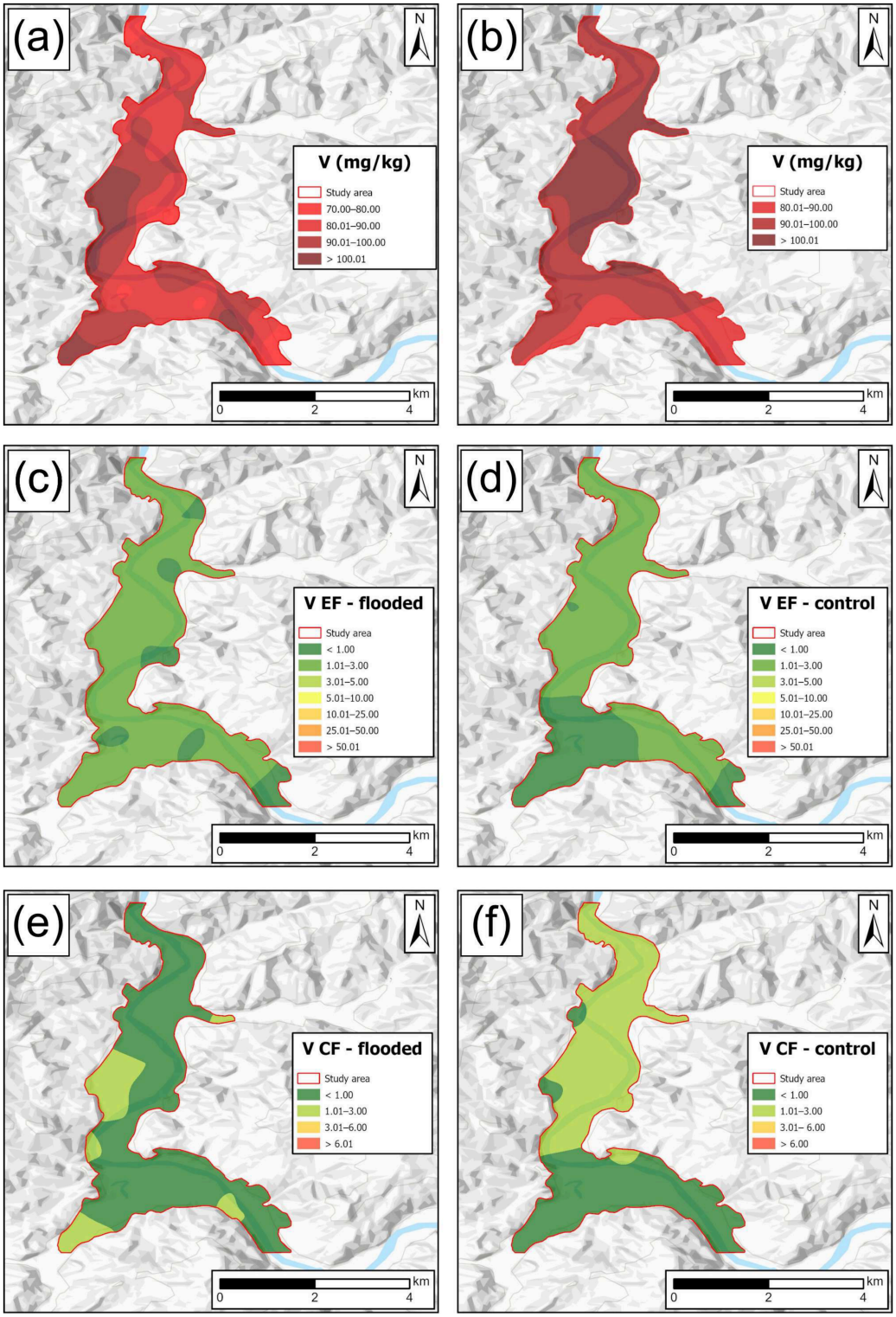

Figure 8. (**a**) Spatial distribution of V in flooded area; (**b**) spatial distribution of V in control area; (**c**) enriched factor for V in flooded area; (**d**) enriched factor for V in control area; (**e**) contamination factor for V in flooded area; (**f**) contamination factor for V in control area.

The enrichment factors (EFs) for Ba and V are classified as minor across almost the entire flooded study area (Figures 7c and 8c), while the control area shows a different distribution (Figures 7d and 8d). The southern part of the control study area is classified as showing no enrichment, whereas the south-west part shows minor enrichment.

The enrichment factors (EFs) of Ba and V in Fluvisols generally indicate minor enrichment, strongly influenced by parent material, i.e., a predominantly geogenic source. Zhou et al. [54] found EF values for V lower than 1.5, indicating that this element is mainly derived from natural processes. In the case of Ba, higher EF values have been observed, suggesting that it can originate from both geogenic sources and anthropogenic inputs, such as emissions from power plants [55].

The contamination factor (CF) was mostly consistent with the EF, indicating that soils in the flooded area are mainly moderately contaminated, while the control study area shows low contamination with Ba (Figure 7e,f). Ba CF values mostly indicate low to moderate contamination relative to local or guideline backgrounds. In a recent floodplain study of the Štiavnica River, Ba was assessed together with Li, Sr, B and V, and contamination factors based on soil guideline values showed moderate contamination by Ba (CF up to about 2.6) [56]. The authors concluded that this contamination could originate mainly from historical mining. In the case of V, there are some differences between CF and EF distribution (Figure 8e,f). According to [57], lower values (close to 1) tend to reflect the natural origin of the elements in the soil.

The Co levels showed extremely high concentrations (45 mg/kg) according to [43] in the north-west part of the flooded area and the north-east part of the control area (Figure 9a,b). The spatial distribution of Co is almost identical in both areas. Similar to previously mentioned PTEs (Cr, Ni, Ba and V), Co is also dominantly geogenic in origin. Cobalt can be inherited from upstream rocks and sediments, especially where the catchment contains ultramafic rocks. In northern Croatia, the high concentrations of cobalt are also controlled by bedrock lithology, with elevated values in Fluvisol soils developed on basic and ultrabasic magmatic rocks [58].

The enrichment factor (EF) for Co is classified as minor across almost the entire flooded study area (Figure 9c), while the control area displays a different distribution (Figure 9d). The northern part of the control study area is classified as having no enrichment, whereas the south-west part shows minor enrichment. This pattern is consistent with the ultramafic lithology of the terrain, where Co exhibits EF values slightly above 1. Low enrichment factors (EF < 3) for Co have also been reported in Fluvisols of the Mitrovica region, Republic of Kosovo, and these appear to be largely related to the parent materials of the soils [59].

The contamination factor (CF) was mostly consistent with the EF, indicating that soils in the flooded and control study areas are low to moderately contaminated with Co (Figure 9e,f). Kanianska et al. [60] also found moderately contaminated Fluvisol soils of the floodplain along the Štiavnica River in central Slovakia with Co.

In this study, Ti-normalised enrichment factors (EFs) were used as a first-order indicator of possible anthropogenic enrichment relative to the local Fluvisol background. Minor EF values (1–3) for most elements indicate that the Bosna River Fluvisols show only slight enrichment compared to control soils; however, interpreting such values in floodplain environments requires caution. EF values between 1 and 3 do not necessarily confirm purely geogenic origins, as they often reflect mixed signals where diffuse anthropogenic inputs including agricultural runoff, atmospheric deposition, and upstream industrial discharges are superimposed on a dominant natural background. Source interpretation therefore relies on the EF in combination with contamination factors, spatial patterns, detailed geological information, and multivariate statistics. The classification of Cr, Ni, Ba, V and Co as predominantly geogenic is supported not only by their generally low to minor EF values but also by their close spatial association with ultramafic and mafic rocks and their clustering with lithogenic elements. Similarly, the inference that Cu, Zn, Pb and Cd have an anthropogenic component is based on slightly elevated EF/CF values, spatial proximity to industrial and agricultural areas, and their joint clustering pattern,

rather than on the EF alone. Nonetheless, some uncertainty remains, and future work integrating sequential extraction, pore-water data, and temporal monitoring after flood events would help to better constrain the relationship between the EF, metal speciation, and actual environmental risk.

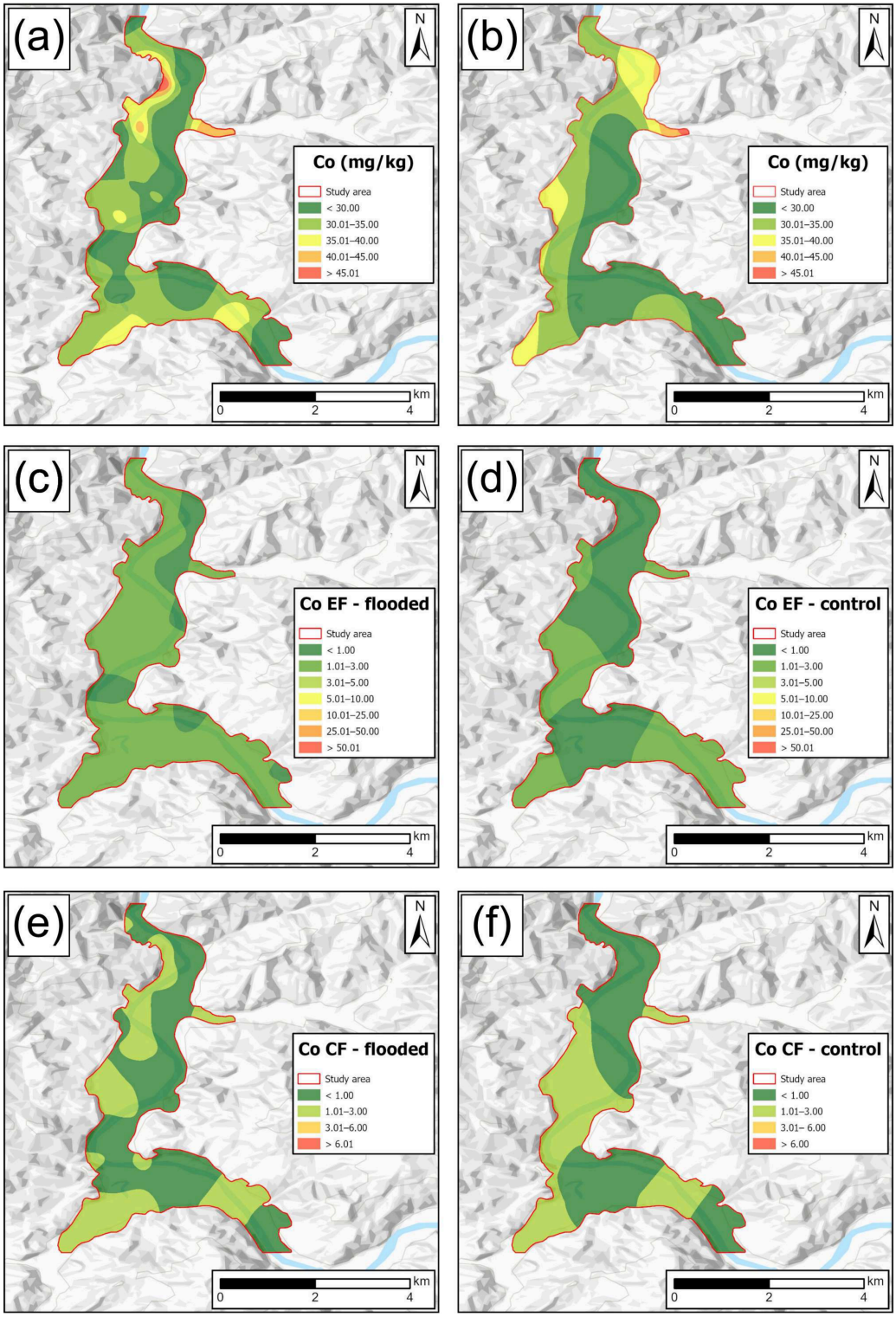

Figure 9. (**a**) Spatial distribution of Co in flooded area; (**b**) spatial distribution of Co in control area; (**c**) enriched factor for Co in flooded area; (**d**) enriched factor for Co in control area; (**e**) contamination factor for Co in flooded area; (**f**) contamination factor for Co in control area.

The EF–CF patterns, together with correlation and cluster analysis, demonstrate that Cr, Ni, Co, Ba and V are elevated but behave consistently with ultramafic and mafic parent rocks, confirming a predominantly geogenic source rather than industrial contamination. In contrast, Cu, Zn, Pb and Cd form coherent spatial clusters, share positive correlations, and show EF values in the minor range, indicating diffuse anthropogenic inputs (industry, agriculture, atmospheric deposition) superimposed on a strong natural background rather than intense point-source pollution. Overall, comparison of flooded and control sites indicates that the flood did not produce a systematic increase in bulk metal concentrations in Fluvisols; instead, flooded sites exhibit enhanced spatial heterogeneity and subtly modified geochemical associations, likely through local erosion–deposition and changes in carbonate- and Fe-oxide-related binding.

3.2. Correlation and Multivariate Statistical Analyses

Average values, standard deviations, and coefficients of variation (Cv) are presented in Appendix A.7. It is clear that for most parameters, average values are very similar. Larger differences are observed for TIC and Ca. When examining standard deviations, more parameters show differences between flooded and control samples, which are more pronounced for Cu, Pb, Zn, Mn, Ba, TIC, TS, Ca, and Mg. In general, this corresponds to the Cv values, with the highest Cv values for gravel, TIC, and TS in flooded samples, and for TIC and Ca in control samples. Higher Cv values for gravel can be expected after flooding. It has been shown that flooding can influence soil texture [61], and that during large floods, suspended sediment quickly becomes saturated, suppressing turbulence and causing rapid, intense deposition of fine gravel and sand [62]. Additionally, it must be emphasised that loss of soil carbon as a consequence of short-duration floods may adversely affect the ecosystem condition of lowland river floodplains [63]. Furthermore, ref. [2] reported that flooding in Fluvisols reduced organic matter content and altered soil chemistry through acidification, redox changes, and washing out of organic fractions. In our study, total inorganic carbon (TIC) relates to available nutrients such as Ca, Na, Mg, and K. This is consistent with [2], which showed that in flooded Fluvisols, total inorganic carbon is biogeochemically linked to base cations such as Ca, Mg, K, and Na because flooding alters pH, redox conditions, mineral dissolution, and solute transport, which in turn affects carbonate behaviour and cation availability.

Correlation matrices are presented in Appendix A Tables A5 and A6. It is clear that flooded samples show more statistically significant results, which suggests that flooding had influence on the observed variables.

Some research has shown that pH can be critical for PTE mobility [64,65]. However, the results in this research do not suggest that, as evidenced by correlation and multivariate analysis (Appendices A.5 and A.6). The only exception is negative correlation between pH and As in the control samples. It has been shown that As concentrations, its distribution and availability, can depend on different factors, from clay content, presence of carbonates, and organic matter to redox condition and pH [66], while some research showed that the influence of soil pH and redox conditions on As bioavailability and bioaccessibility should be investigated in more detail in future research [67]. Other research found that pH influence on As availability is higher with respect to the OM in the dryland, but less in the paddy fields [68]. Additionally, it was found that soil organic carbon and total concentration present dominant drivers of metal mobility, with soil pH positively correlated with the mobile As fraction. Furthermore, it was shown that low to moderate organic carbon (<2%) and slightly acidic pH can reduce As mobility, which is especially pronounced in the clay-rich soils [69]. This is consistent with the results of this research, i.e., elevated As concentrations, in soils without clay, neutral pH and organic content higher than 2% in

most of the cases for both flooded and control samples. These results are in line with the spatial distribution and geochemical factors, which implies that the observed As behaviour is largely controlled by its geogenic origin, whereby weathering of As-bearing minerals supplies arsenic that is subsequently redistributed through pH and complexation with soil organic matter, and redox-driven transformations between As(III) and As(V) that jointly regulate its mobility and availability in Fluvisol soils. In contrast, elevated OM values in soils increase the immobility of metals, as evidenced by a positive correlation between TOC values and several PTEs. It should be emphasised that in the flooded samples, a statistically significant positive correlation between pH and Ba was observed. Ba in soil generally shows a positive correlation with soil pH, meaning that as soil pH increases, the concentration of bioavailable barium tends to increase. Although the difference is small, a slightly higher average pH has been recorded in the flooded samples, which is consistent with the correlation analysis. Correlation analysis of soil texture variables did not reveal many statistically significant correlations in either data set. In the flooded samples, silt was positively correlated with As, while sand was negatively correlated with Cu, Zn, and Cd; this negative correlation was also evident between gravel and Zn. In the control samples, only gravel was negatively correlated with As. Additionally, in the flooded samples, sand was negatively correlated with TC, TIC, and TOC, although the correlation with TIC was not statistically significant. In contrast, in the flooded samples, gravel was positively correlated with TC, TIC, and TOC (not statistically significant), and negatively correlated with pH. In the control samples, a different correlation of gravel with TOC and pH was observed: gravel was negatively correlated with TOC and positively correlated with pH. Although it has been shown that organic matter can be influenced by soil texture [70,71], these results also suggest that flood-affected sites display different relationships between gravel, TOC, and pH compared to control sites.

It is clear that PTEs such as Mo, Cu, Pb, Fe, Zn, As, Cd, and Ba are negatively correlated with Na in the flooded samples, a pattern that is less pronounced in the control samples, except for Cu, Pb, and Li. This suggests that flooding influenced the concentrations of PTEs. It has been shown that cations can compete with heavy metal ions for adsorption sites [72], which ultimately promotes the desorption of heavy metal ions from the soil and increases their soluble activity [73]. Some research has shown that increasing salinity can enhance the migration rates of Cd, Mn, Cu, and Pb in sediments [74]. It is known that sodium concentration regulates the mobility of PTEs, and their correlation is usually positive. Additionally, some studies suggest that siderite, which is usually associated with trace elements such as Ni, Mn, Co, Pb, and Zn, can release various heavy metals during weathering. In alluvial soils, these elements can precipitate and accumulate under anoxic conditions [57].

Cu, Pb and Zn are mutually positively correlated in both sets, suggesting a common origin, probably natural, with possible minor anthropogenic influence indicated by slightly elevated EFs. Additionally, they all are positively correlated with Mo in the flooded samples. Van et al. [75] noted that recent research indicates Zn contamination can result from excessive use of Zn-based fertilisers and industrial activities. Tang et al. [76] showed that coal production can be the most important source of Cd, Zn and Cu, while [77] stated that anthropogenic sources of Cd in soils are related to the direct input of waste material from mining, industry and agriculture. However, cluster analysis results indicate differences between the two sets of samples (Figure 10). Cluster analysis defined five and six clusters for flooded and control samples, respectively, which is consistent with the number of extracted factors. It should be emphasised that factor analysis for flooded samples explained 77.17% of the total variance, while in control samples it explained 94.06%. In many cases, the results of both multivariate analyses coincide. However, factor

analysis highlights relationships that are more relevant and should be the focus of data interpretation. In the flooded samples, Cu, Pb and Zn belong to the same cluster, together with Cd and Mo (which is generally consistent with their mutual positive correlation), while in the dendrogram for the control samples, they belong to different clusters (Figure 11). This is also partially consistent with the factor analysis for flooded samples, where Pb, Zn and Cd belong to the same factor, together with Na. In contrast, in control samples, Cu belongs to the first factor together with Fe, Cd, V and Al, while Zn shows significant loading in factor 4 (Figures 12 and 13, Appendices A.8–A.11). This suggests that flood-affected sites display modified associations of Cu, Pb and Zn compared to control sites, which is consistent with the observed differences in their spatial distribution between flooded and unflooded areas. In factor analysis of control samples, Mo and Pb do not show significant loading in any factor. This is not consistent with the cluster analysis results, where Pb is grouped with lithogenic elements such as Li, Ba, Zr and Mo. The reason for the grouping of Pb in cluster analysis is probably related to a geogenic or natural source in soils, where the parent material is ultramafic rocks. This aligns with the research of [78], where Pb is reported as part of natural geochemical associations rather than purely anthropogenic contamination, depending on local lithology and weathering regime. In cluster analysis of the control samples, Cu is grouped with V, Al, Fe, Mn, Cd and sand, which implies it may covary with Fe and Mn due to adsorption onto oxide phases, and with Al or V when controlled by lithology and fine particles, while co-variation with Cd can occur but often reflects mixed natural and anthropogenic inputs. This is consistent in some part with the results of the factor analysis where Cu belongs to the same factor as Fe, Cd, V and Al.

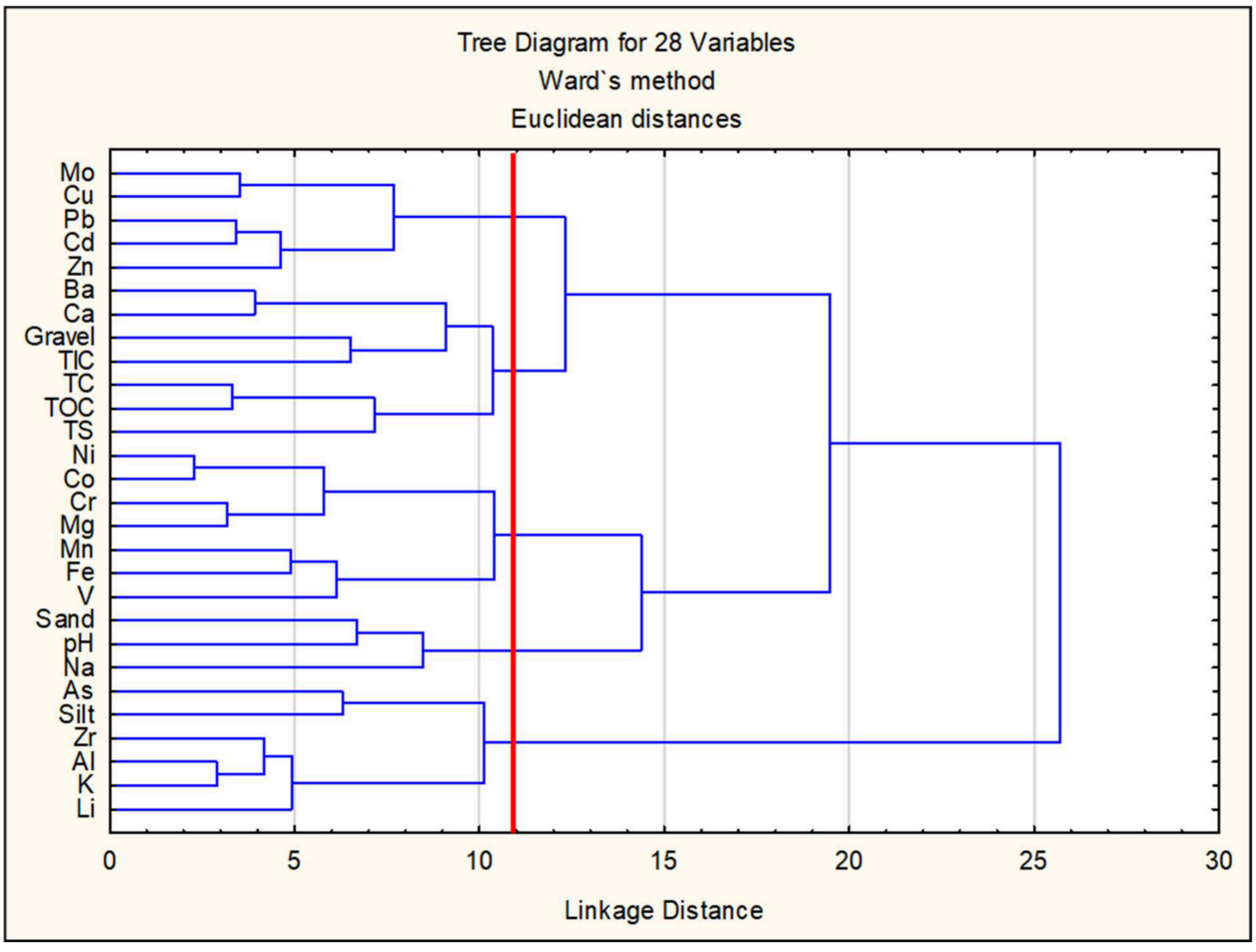

Figure 10. Dendrogram for flooded samples. Red line represents a cut-off line for cluster identification.

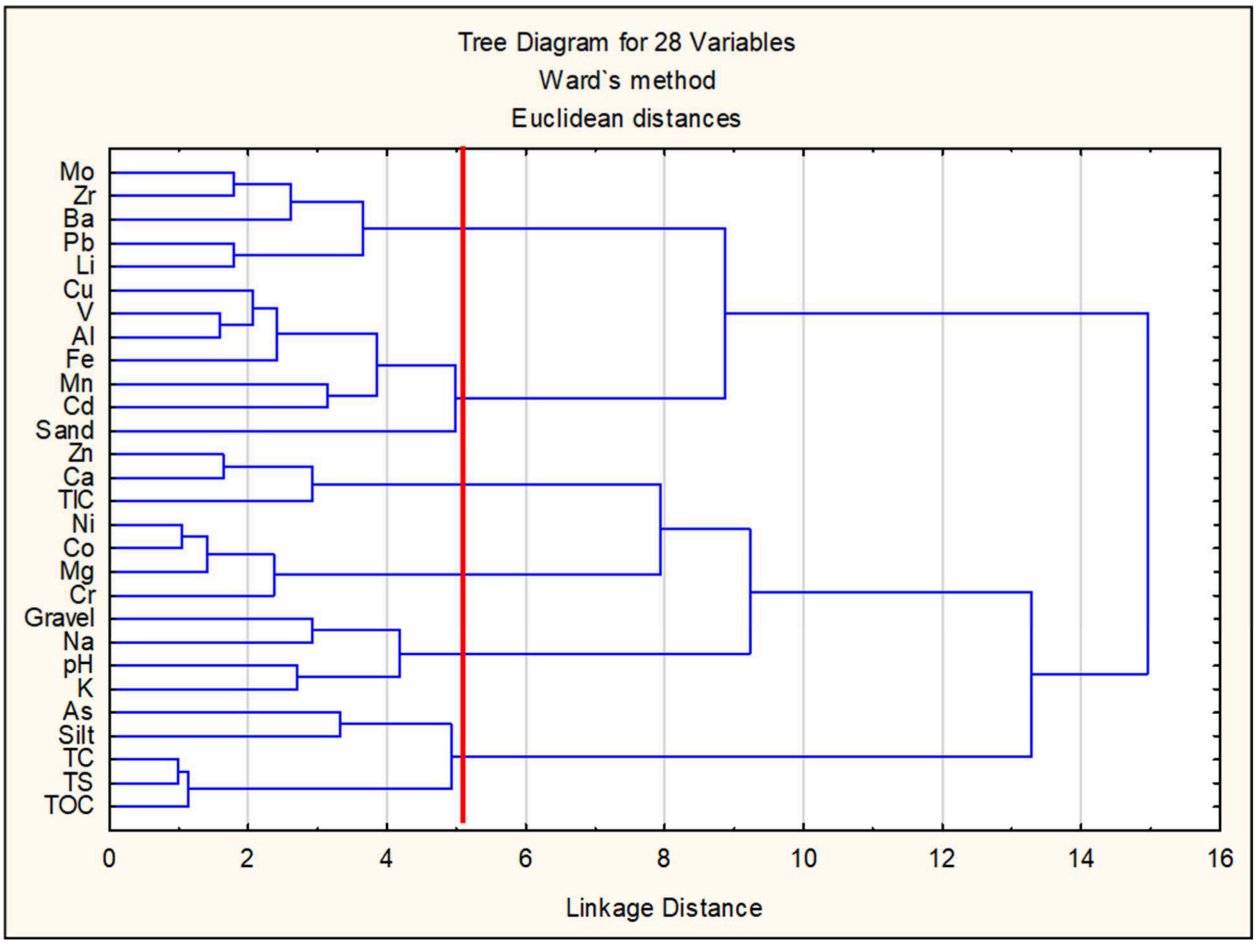

Figure 11. Dendrogram for control samples. Red line represents a cut-off line for cluster identification.

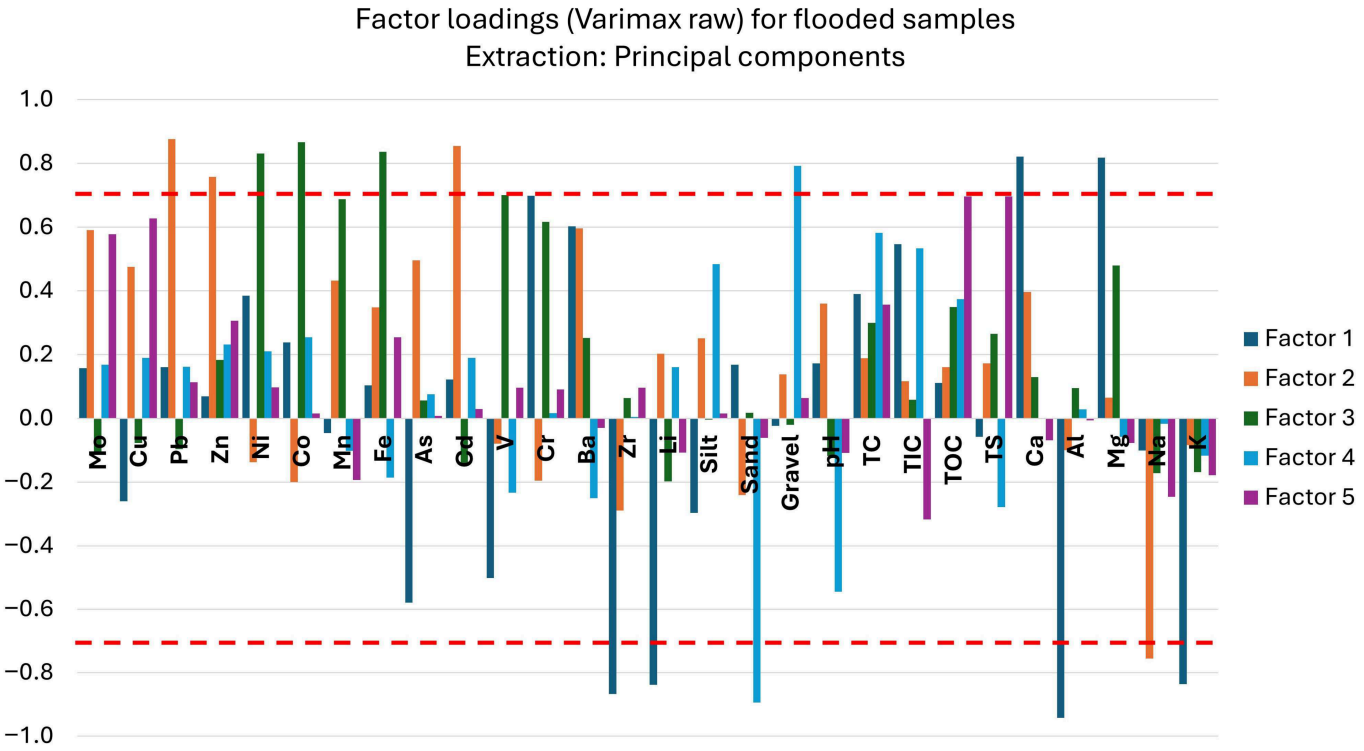

Figure 12. Factor loadings in flooded samples. Stippled red line presents an area with factor loadings greater than 0.7 in magnitude.

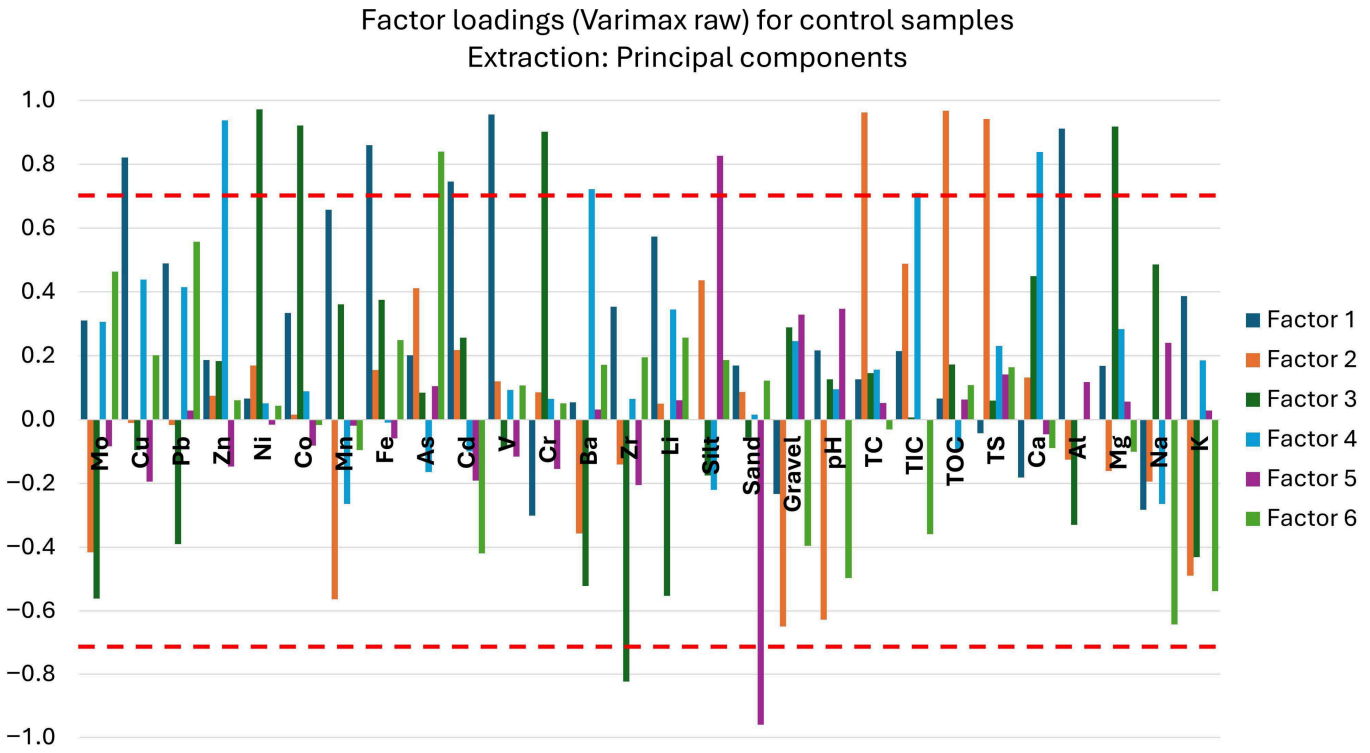

Figure 13. Factor loadings in control samples. Stippled red line presents an area with factor loadings greater than 0.7 in magnitude.

In the cluster analysis of control samples, Zn is grouped with Ca and TIC, which can be explained geogenically, which corresponds to the results of the factor analysis where Zn is grouped with Ba, TIC and Ca in factor 4. Increasing pH and carbonate content reduces Zn solubility and favours Zn retention in the solid phase, making Zn appear more closely linked to Ca-bearing inorganic carbon fractions.

Additionally, ref. [77] stated that Cd leaching from various contamination sources can occur when Cd release is promoted by replacement, formation of soluble complexes, acidification, or oxidation, which can happen during flooding and may explain differences in the spatial distribution of Cd concentrations before and after flooding (Appendix A.1). Furthermore, the positive, though weak, correlation between Cd and Ca in flooded samples supports this interpretation, as Cd can replace Ca during mineral formation and co-precipitation. This correlation is not observed in the control samples. It is notable that Cd in flooded samples does not show the same positive correlation with Mn and Fe as seen in control samples, which is the opposite of the correlation between Cd and Zn. This is inconsistent with research indicating that both Mn and Zn play crucial roles in suppressing Cd accumulation in both acidic and alkaline soils [79]. However, the statistically significant positive correlation between Cd and Fe in control samples, along with lower concentrations, may indicate binding of Fe oxides to Cd, which may have acted as an immobilisation mechanism, resulting in lower solubility and mobility of Cd before flooding. This is consistent with the cluster analysis, where Cd was grouped with Fe before flooding. In contrast, factor analysis of flooded samples suggests grouping of Cd with Na, which requires further investigation in future research.

Potassium is negatively correlated with Ni, Co, Cr, and Ba in flooded samples, while in the control samples, a statistically significant negative correlation is observed only with Cr. Some studies have shown that potassium fertilisation increases Cd and Pb concentrations and reduces Cr and Fe concentrations in soil [80], while others have found that ultramafic soils are characterised by high concentrations of Ni, Cr, and Co, which may be related to the

rock chemistry, including a deficiency of plant-essential nutrients, especially potassium and nitrogen [81]. Cluster analysis performed on control samples suggests grouping with pH, Na, and gravel, while factor analysis does not indicate significant loading in any factors. Both multivariate analyses generally coincide regarding the grouping of potassium in flooded samples; in cluster analysis, it is grouped with As, silt, Zr, Al, and Li, while in factor analysis, it belongs to factor 1 together with Zr, Li, Ca, Al, and Mg.

Magnesium is moderately to strongly positively correlated with Ni, Co, and Cr in both sets of samples, suggesting that it plays a significant role in their behaviour. This also indicates that their concentrations can naturally originate from ultramafic and serpentinite rocks, which is consistent with the negative correlation with potassium. It has been shown that high concentrations of Co, Cr, and Ni in serpentinite soil can be related to the high content of ferromagnesian minerals in the rocks, in which Ni, Cr, and Co substitute for Mg and Fe (Al) [82]. The influence of magnesium on Ni, Cr, and Co is also confirmed through cluster analysis in both cases (Figures 10 and 11). However, it must be emphasised that the process of pedogenesis can also generate different patterns of Ni, Cr, and Co concentrations [83]. When inspecting the correlation between Ni, Cr, and Co, the correlation values are positive. All these findings, together with EFs, confirm that the concentrations of Ni, Cr (although elevated), and Co are predominantly of natural origin, while the spatial patterns of their concentrations suggest that flooding did not have much influence on their distribution. This is consistent with the results of cluster analysis, where Mg is grouped with Ni, Co, and Cr. Factor analysis produced different results where Mg is grouped with Ni, Co, Cr, and Zr in factor 3, while for flooded samples it belongs to factor 1, together with other lithogenic elements.

Concentrations and their spatial distribution suggest that flooding had a minor influence on Ba and V concentrations. Although high, it is possible that most concentrations are generally related to geogenic origin. In flooded samples, Ba has a positive correlation with Pb, Zn, Mn, Fe, Cd, Cr, pH, Ca, and Mg, and a negative correlation with Zr, Li, Al, Na, and K. In control samples, Ba only has statistically significant positive correlations with Mo and Pb. Taking this into account, it is clear that flooding influenced Ba concentrations. This is consistent with the cluster analysis, where in control samples Ba is grouped with Mo, Zr, Pb, and Li, while in flooded samples Ba is clustered with Ca, then gravel, carbon, and sulphides. Factor analysis performed on the flooded samples does not suggest any significant loading, while in control samples it is grouped in factor 4 together with Zn, TIC, and Ca. Previous research showed that calcium carbonate, cation exchange capacity, and pH can be the most important soil properties influencing the transfer of Ba into groundwater [84,85]. It was also found that in the aquatic environment Ba is prone to precipitate as insoluble salts such as $BaSO_4$ and $BaCO_3$ [86].

Vanadium is positively correlated with Cu, Pb, Fe, Cd, Li, and Al in control samples, with no significant negative correlation parameters. In contrast, in the flooded samples, it is positively correlated with Co, Fe, Zr, and Al, and negatively correlated with Cd and TIC. This suggests that, in most cases, V concentrations are related to Fe and Al concentrations, which is largely consistent with the results of the cluster and factor analyses, where V is in the same cluster and factor as Fe and Al in control samples, and with Fe in flooded samples. It has been shown that microbial Fe(III) reduction can be a very important factor related to V(V) release and reduction [87], while [88] found that Fe-Mn-modified biochar can achieve significantly higher passivation effects and reduce the bioavailability of Ti, V, and As. Additionally, it is known that V behaviour in soil is usually linked with soil organic matter and aluminium and iron oxides [89]. After flooding, it is possible that Al is linked with Fe and Mn due to redox-driven dissolution and reprecipitation of Fe/Mn oxides, which reorganised the reactive soil matrix. These same fine particles and oxide redistribution

promoted co-association of Al with Li and, to a lesser extent, K, which primarily reflected the inherited aluminosilicate fraction [90].

Our data indicate that the flood primarily modified the mobility and spatial distribution of selected PTEs rather than causing uniformly higher contamination levels. In flooded Fluvisols, negative correlations between Na and Zn, As and Cd, the distinct clustering of Cu, Pb, and Zn with Cd and Mo, and the differences in Cd–Fe associations relative to control soils collectively suggest that flooding enhanced the redistribution and, for some elements, the mobility of metals such as Zn, As and Cd. At the same time, the predominance of low to moderate EF and CF classes and the continued importance of carbonate and organic matter controls (e.g., Zn association with Ca–TIC and positive correlations between TOC and several PTEs) imply that geogenic background, carbonate buffering and organic complexation still exert strong constraints on metal bioavailability in the Bosna River Fluvisols.

4. Conclusions

This study demonstrates that Bosna River Fluvisols are generally slightly to moderately contaminated by potentially toxic elements (PTEs), with most elements exceeding guideline values only in limited areas and EF/CF values predominantly in low classes. This indicates that natural lithology and soil properties exert a strong influence, rather than widespread severe pollution. Elements such as Cr, Ni, Co, Ba, and V are elevated but display patterns consistent with ultramafic and mafic parent rocks, as evidenced by positive correlations with Mg and Fe, low EF values, and stable spatial distributions between flooded and control sites, confirming their predominantly geogenic origin.

Overall, the combined EF–CF patterns, spatial distributions, and multivariate statistics indicate that sites affected by the flood display primarily featured altered spatial distribution and associations of PTEs compared to control sites, rather than representing a uniformly more contaminated system. Arsenic, Cu, Zn, Pb, and Cd require targeted monitoring due to their elevated concentrations and flood-sensitive behaviour. The integrated use of Ti-normalised EF referenced to local Fluvisol background, GIS mapping, and comparative flooded-versus-control multivariate analysis provides a robust and transferable framework for post-flood source apportionment and risk assessment in other alluvial plains with naturally high metal contents.

Future research should incorporate time-series sampling (pre- and post-flood), sediment core stratigraphy, and hydrodynamic sediment transport modelling to better constrain how extreme floods govern the vertical and lateral redistribution, phase partitioning, and bioavailability of PTEs in Fluvisols.

Author Contributions: Conceptualization, S.R., E.B., S.U. and A.B.; methodology, M.C., T.B., S.U., A.B., S.R. and E.B.; software, Z.K. and T.B.; validation, Z.K. and T.B.; formal analysis, M.C., S.U., E.B. and A.B.; investigation, S.U., E.B. and A.B.; resources, E.B. and A.B.; data curation, Z.K., M.C., S.U., E.B. and A.B.; writing—original draft preparation, S.R., T.B., Z.K., E.B. and M.C.; writing—review and editing, S.R., T.B., Z.K., E.B. and M.C.; visualisation, S.R., T.B., Z.K., E.B. and M.C.; supervision, S.R. and E.B.; project administration, E.B. and A.B.; funding acquisition, S.R., T.B. and E.B. All authors have read and agreed to the published version of the manuscript.

Funding: This research received no external funding.

Data Availability Statement: Data is available in Appendix A.

Conflicts of Interest: The authors declare no conflict of interest.

Abbreviations

The following abbreviations are used in this manuscript:

PTE	Potentially toxic element
EF	Enrichment factor
CF	Contamination factors
TC	Total carbon
TIC	Total inorganic carbon
TOC	Total organic carbon
TS	Total sulfur

Appendix A

Appendix A.1

Table A1. Total concentration of elements. All elements are expressed in mg/kg, except Ca, K, Na, Mg, Al and Fe, which are expressed in %.

Sample	Mo	Cu	Pb	Zn	Ni	Co	Mn	Fe	As	Cd	V	Cr	Ba	Zr	Li	Ca	Al	Mg	Na	K
1	0.64	34.80	50.89	145.90	310.40	31.00	1156.00	3.64	14.00	0.37	79.00	585.00	468.00	40.10	29.40	5.61	4.24	3.58	0.76	0.90
2	0.59	35.90	47.34	129.80	348.10	33.40	1219.00	4.03	13.00	0.23	91.00	607.00	514.00	43.80	32.40	3.76	4.59	3.78	0.80	0.98
3	0.39	41.40	68.24	117.30	215.00	25.40	1289.00	3.60	22.70	0.43	85.00	411.00	496.00	56.50	40.00	2.01	5.29	1.99	0.83	1.24
4	0.50	48.20	50.57	134.80	504.50	49.70	1439.00	4.39	18.70	0.40	91.00	766.00	451.00	48.10	34.60	2.05	5.36	3.42	0.74	1.04
5	0.75	39.70	52.32	148.40	265.50	30.40	1347.00	4.10	15.70	0.40	90.00	457.00	531.00	46.30	35.40	3.56	5.04	3.03	0.76	1.18
6	0.35	40.80	43.48	96.50	214.20	26.50	1226.00	3.46	20.00	0.39	82.00	385.00	357.00	46.60	36.40	1.90	4.98	1.97	0.81	1.17
7	0.35	32.90	32.30	82.60	173.40	19.00	773.00	3.13	12.80	0.12	87.00	356.00	284.00	55.10	42.40	0.76	5.42	1.37	0.92	1.21
8	0.64	37.80	43.53	122.10	452.60	42.60	1298.00	4.62	11.50	0.28	95.00	954.00	593.00	42.50	26.30	3.85	4.36	4.98	0.71	0.89
9	0.46	48.00	40.80	113.50	199.30	24.30	1111.00	3.52	18.20	0.40	85.00	357.00	372.00	48.30	37.60	1.33	5.40	1.54	0.83	1.32
10 *	0.94	57.20	33.10	93.20	103.50	21.90	1488.00	3.79	15.00	0.15	106.00	154.00	326.00	86.10	58.90	0.37	6.60	0.98	0.64	1.80
11	0.81	64.80	55.51	159.20	211.00	27.60	1531.00	3.90	21.50	0.46	96.00	284.00	407.00	60.80	54.90	2.36	5.95	1.69	0.76	1.46
12	0.15	33.20	14.60	59.00	368.70	41.00	1223.00	3.65	8.50	0.10	96.00	597.00	167.00	59.30	31.90	2.23	5.32	3.47	1.44	1.17
13 *	0.47	50.10	30.62	97.70	387.20	42.90	1761.00	4.29	16.10	0.27	105.00	595.00	266.00	60.30	44.40	1.06	5.96	2.78	1.12	1.28
14	0.84	70.70	62.71	149.60	284.20	30.60	1351.00	4.43	15.50	0.54	89.00	524.00	690.00	46.20	30.70	3.68	4.86	3.24	0.75	1.14
15	0.48	48.00	38.90	108.60	233.60	24.80	988.00	3.84	17.20	0.27	95.00	438.00	319.00	59.80	40.10	1.10	5.86	1.44	0.86	1.35
16	0.52	46.00	44.41	130.40	268.40	31.30	1317.00	4.34	15.90	0.25	98.00	490.00	514.00	55.20	33.90	3.71	5.24	3.15	0.80	1.23
17	0.57	37.00	41.83	130.00	350.10	32.60	1264.00	4.22	12.60	0.31	88.00	691.00	600.00	38.40	26.90	4.70	4.33	3.95	0.71	0.93
18 *	0.48	48.40	34.10	87.80	176.60	22.70	962.00	3.71	20.50	0.17	101.00	285.00	283.00	69.10	64.60	0.45	6.08	0.96	0.62	1.28
19	0.39	43.50	43.01	108.90	203.60	26.00	1162.00	3.68	17.20	0.21	97.00	353.00	384.00	62.70	41.80	1.72	5.74	1.87	0.93	1.23
20	0.66	37.10	46.98	147.50	315.40	32.80	1277.00	4.34	13.60	0.31	94.00	578.00	548.00	43.30	29.40	4.05	4.61	3.65	0.78	1.03
21	0.52	41.80	42.92	112.00	351.40	34.60	1428.00	3.94	15.50	0.27	89.00	664.00	537.00	46.40	29.80	3.20	4.64	3.51	0.79	1.01
22	0.50	42.90	38.37	108.70	246.90	28.40	1270.00	3.93	16.70	0.28	89.00	433.00	407.00	52.80	37.30	2.38	5.38	2.10	0.79	1.30
23 *	0.22	34.60	23.04	68.60	226.20	27.30	1253.00	3.29	7.40	0.17	85.00	364.00	246.00	61.70	34.20	0.57	5.76	1.64	1.48	1.57
24	0.38	32.20	30.21	76.10	222.50	27.10	1046.00	3.09	8.40	0.19	79.00	370.00	316.00	53.70	34.60	1.04	5.57	1.78	1.47	1.46
25	0.40	46.50	28.79	89.70	284.90	34.40	1537.00	4.24	17.60	0.22	101.00	467.00	303.00	60.20	36.50	0.73	5.91	1.48	0.90	1.38
26	0.41	47.90	28.93	87.80	364.60	36.40	1425.00	4.44	18.40	0.19	101.00	464.00	261.00	55.70	37.90	0.80	5.98	1.59	0.83	1.38
27	0.40	41.20	43.92	109.30	221.60	29.80	1274.00	3.39	18.30	0.34	78.00	378.00	368.00	48.70	35.90	1.98	5.13	1.75	0.76	1.20
28	0.50	41.00	43.01	110.80	246.00	28.70	1173.00	3.56	16.50	0.29	80.00	409.00	327.00	56.90	30.60	1.85	5.15	1.96	0.77	1.19
29 *	0.29	47.10	27.67	96.00	287.00	32.10	1318.00	3.86	16.50	0.22	92.00	482.00	250.00	58.70	39.70	1.44	5.75	1.94	0.87	1.25
30 *	0.34	37.20	26.97	77.20	195.80	23.50	860.00	3.13	10.40	0.18	87.00	445.00	260.00	68.50	40.70	0.51	5.26	1.02	0.98	1.24
31	0.47	39.50	24.81	77.90	238.50	33.20	1207.00	3.81	27.90	0.04	99.00	484.00	218.00	64.60	37.20	0.47	5.33	1.25	0.89	1.15
32 *	0.45	43.00	28.31	81.50	301.10	31.20	937.00	3.92	27.80	0.09	93.00	452.00	241.00	67.30	38.50	0.76	5.60	1.51	0.85	0.99
33	0.21	47.30	25.55	102.50	320.60	34.90	993.00	3.52	10.50	0.16	93.00	492.00	261.00	60.00	39.30	1.19	5.54	1.85	1.06	1.36
34	1.58	108.60	55.22	144.80	253.90	27.30	1140.00	3.79	16.40	0.48	77.00	455.00	319.00	46.20	32.20	2.58	4.82	1.56	0.73	1.02
35	0.55	53.70	38.21	152.20	411.50	35.70	1441.00	4.73	21.40	0.22	105.00	508.00	435.00	57.80	35.40	1.51	6.07	2.15	0.72	1.33
36	0.46	45.60	63.34	161.50	268.70	30.40	1364.00	4.00	16.90	0.28	85.00	486.00	610.00	49.70	32.30	3.44	5.01	2.75	0.73	1.20
37	0.95	75.30	66.96	224.70	277.90	29.80	1078.00	4.24	22.60	0.43	102.00	294.00	337.00	61.80	49.50	1.45	5.88	1.68	0.60	1.21
38	0.50	38.70	38.59	94.10	198.20	24.80	1084.00	3.39	18.70	0.26	85.00	314.00	345.00	48.80	38.00	2.03	5.03	1.63	0.81	1.27
39	0.48	54.20	38.11	113.40	219.70	30.30	1303.00	3.80	19.40	0.32	98.00	328.00	363.00	61.10	42.50	0.82	5.73	1.22	0.85	1.35
40	0.54	48.90	48.99	127.50	275.70	32.10	1370.00	3.89	19.00	0.39	89.00	348.00	381.00	55.20	38.20	2.23	5.70	2.07	0.76	1.34
41 *	0.21	51.00	24.68	87.30	317.00	36.70	1507.00	4.00	16.00	0.25	99.00	408.00	219.00	60.70	47.00	0.80	5.93	1.85	0.96	1.52
42 *	0.40	55.30	30.65	93.90	258.40	32.40	1335.00	4.40	16.60	0.40	117.00	339.00	256.00	72.00	52.10	0.75	6.57	1.63	0.92	1.45
43 *	0.39	54.00	30.55	96.80	250.00	32.40	1305.00	4.35	16.40	0.30	112.00	363.00	249.00	71.30	53.10	0.74	6.38	1.57	0.85	1.40
44	0.44	52.40	30.05	137.10	290.30	32.90	830.00	3.63	12.10	0.16	95.00	459.00	312.00	64.50	50.90	2.63	5.63	2.12	0.90	1.45
45	0.48	45.30	56.43	109.70	230.10	27.10	1246.00	3.57	24.30	0.39	87.00	305.00	360.00	47.90	41.30	2.33	5.45	1.93	0.76	1.34
Flooded	Mo	Cu	Pb	Zn	Ni	Co	Mn	Fe	As	Cd	V	Cr	Ba	Zr	Li	Ca	Al	Mg	Na	K
Average	0.54	46.78	43.82	120.20	280.90	31.00	1245.59	3.89	16.97	0.30	90.44	471.53	407.15	52.37	36.25	2.31	5.26	2.36	0.84	1.20
Stdev	0.25	14.69	12.29	31.48	76.84	5.79	162.76	0.41	4.29	0.11	7.50	145.76	122.35	7.15	5.96	1.26	0.50	0.97	0.18	0.16
CV	0.45	0.31	0.28	0.26	0.27	0.19	0.13	0.11	0.25	0.38	0.08	0.31	0.30	0.14	0.16	0.55	0.10	0.41	0.21	0.13
Control	Mo	Cu	Pb	Zn	Ni	Co	Mn	Fe	As	Cd	V	Cr	Ba	Zr	Li	Ca	Al	Mg	Na	K
Average	0.42	48.21	29.07	92.46	253.92	30.55	1232.36	3.85	15.89	0.21	99.27	395.09	264.36	67.29	47.65	0.92	5.96	1.64	0.93	1.38
Stdev	0.20	7.27	3.35	17.39	76.92	6.34	300.78	0.41	5.31	0.09	10.11	115.28	31.45	7.76	9.28	0.64	0.42	0.54	0.23	0.21
CV	0.47	0.15	0.12	0.19	0.30	0.21	0.24	0.11	0.33	0.40	0.10	0.29	0.12	0.12	0.19	0.70	0.07	0.33	0.25	0.15

* Control samples.

Appendix A.2

Table A2. Soil physical and chemical parameters. Units are expressed in %.

Sample	Silt	Sand	Gravel	pH	TC	TIC	TOC	TS
1	9.36	69.09	21.55	7.07	4.49	2.17	2.31	0.00
2	8.54	88.19	3.27	7.03	2.69	0.74	1.95	0.00
3	9.66	88.57	1.77	7.15	2.53	0.64	1.89	0.00
4	15.28	73.42	11.30	6.78	5.22	1.75	3.47	0.00
5	9.14	89.53	1.33	7.46	2.59	0.91	1.68	0.03
6	8.21	90.52	1.28	7.18	2.06	0.14	1.92	0.00
7	9.17	89.91	0.92	7.14	1.07	0.04	1.04	0.00
8	6.01	91.59	2.40	6.97	3.63	0.21	3.42	0.05
9	9.58	88.81	1.61	7.05	0.41	0.00	0.41	0.00
10 *	8.71	84.77	6.53	7.24	1.04	0	1.04	0.02
11	8.27	76.51	15.22	7.06	1.18	0.00	1.18	0.02
12	8.81	90.65	0.55	7.08	1.56	0.29	1.27	0.00
13 *	9.12	82.35	8.54	7.45	1.86	0	1.86	0.02
14	8.87	90.41	0.72	7.74	2.50	0.00	2.50	0.04
15	3.17	88.36	8.47	7.24	2.53	0.15	2.38	0.03
16	8.77	89.04	2.19	7.61	3.19	0.46	2.73	0.04
17	9.48	89.84	0.69	7.37	2.26	0.16	2.10	0.03
18 *	19	77.04	3.96	7.12	3.06	0	3.06	0.05
19	9.00	88.26	2.74	7.06	2.86	0.10	2.76	0.04
20	8.18	89.94	1.88	7.31	2.48	0.99	1.48	0.04
21	6.52	92.64	0.84	7.11	3.72	1.10	2.61	0.05
22	7.44	87.94	4.62	7.24	3.05	0.88	2.17	0.03
23 *	15.33	72.49	12.18	7.45	1.89	0	1.89	0.02
24	9.52	83.27	7.21	7.15	2.47	0.62	1.85	0.02
25	9.66	88.91	1.43	7.04	2.60	0.44	2.16	0.02
26	5.37	91.70	2.93	7.20	2.23	0.01	2.22	0.03
27	9.70	83.28	7.03	7.24	3.33	0.57	2.76	0.04
28	9.07	84.85	6.08	7.11	3.14	0.39	2.76	0.04
29 *	9.24	80.96	9.8	6.98	2.47	0	2.47	0.03
30 *	6.88	89.09	4.03	6.95	2.44	0	2.44	0.03
31	12.22	86.60	1.18	7.02	2.19	0.00	2.19	0.03
32 *	16.23	81.67	2.1	6.63	3.58	0	3.58	0.05
33	8.31	80.91	10.78	6.44	2.29	0.00	2.29	0.03
34	12.09	77.85	10.06	7.18	3.85	0.33	3.52	0.04
35	9.07	81.35	9.58	7.24	2.70	0.00	2.70	0.06
36	6.21	89.03	4.76	6.91	3.03	0.62	2.41	0.05
37	15.32	77.16	7.52	6.58	3.74	0.18	3.56	0.05
38	9.17	89.79	1.04	7.10	2.68	1.16	1.52	0.03
39	17.13	79.90	2.97	7.34	2.22	0.01	2.21	0.03
40	13.53	82.73	3.75	7.19	2.31	0.11	2.20	0.03
41 *	10.31	85.53	4.16	7.24	2.98	0	2.98	0.04
42 *	13.9	83.43	2.67	7.06	4.45	0.74	3.72	0.05
43 *	8.95	84.96	6.09	6.92	2.56	0	2.56	0.03
44 *	9.55	81.99	8.46	7.13	3.48	0.82	2.66	0.05
45	14.39	80.89	4.72	7.45	3.51	0.67	2.83	0.04
Flooded	Silt	Sand	Gravel	pH	TC	TIC	TOC	TS
Average	9.54	85.63	4.84	7.14	2.72	0.47	2.25	0.03
Stdev	2.93	5.81	4.77	0.25	0.94	0.52	0.72	0.02
Cv	0.31	0.07	0.99	0.03	0.35	1.12	0.32	0.64
Control	Silt	Sand	Gravel	pH	TC	TIC	TOC	TS
Average	11.56	82.21	6.23	7.11	2.71	0.14	2.57	0.04
Stdev	3.88	4.44	3.20	0.24	0.94	0.32	0.78	0.01
Cv	0.34	0.05	0.51	0.03	0.35	2.23	0.30	0.33

* Control samples.

Appendix A.3

Table A3. Enrichment factors (EFs) of selected elements.

Sample	Mo	Li	As	Pb	Cd	Cu	Cr	Ni	Zn	Co	Ba	V
1	2.16	0.87	1.24	2.48	2.49	1.02	2.09	1.73	2.24	1.41	2.50	1.13
2	1.77	0.86	1.02	2.06	1.38	0.94	1.94	1.73	1.78	1.36	2.45	1.16
3	1.10	0.99	1.67	2.77	2.42	1.02	1.23	1.00	1.50	0.96	2.21	1.01
4	1.49	0.90	1.46	2.17	2.38	1.25	2.42	2.47	1.82	2.00	2.13	1.14
5	2.18	0.90	1.19	2.19	2.32	1.01	1.41	1.27	1.96	1.19	2.45	1.11
6	1.04	0.95	1.55	1.86	2.31	1.06	1.21	1.05	1.30	1.06	1.68	1.03
7	0.92	0.98	0.88	1.23	0.63	0.76	0.99	0.75	0.99	0.68	1.19	0.97
8	1.94	0.70	0.91	1.90	1.69	1.00	3.06	2.26	1.68	1.74	2.85	1.22
9	1.30	0.93	1.35	1.67	2.26	1.18	1.07	0.93	1.46	0.93	1.67	1.02
10 *	2.17	1.20	0.91	1.10	0.69	1.15	0.38	0.39	0.98	0.68	1.19	1.04
11	2.11	1.26	1.46	2.09	2.39	1.47	0.78	0.91	1.89	0.97	1.68	1.06
12	0.42	0.79	0.63	0.59	0.56	0.82	1.79	1.71	0.76	1.56	0.75	1.15
13 *	1.08	0.90	0.97	1.02	1.25	1.01	1.46	1.47	1.03	1.34	0.97	1.03
14	2.28	0.73	1.10	2.46	2.93	1.68	1.51	1.27	1.85	1.12	2.98	1.02
15	1.22	0.90	1.15	1.43	1.38	1.07	1.18	0.98	1.26	0.85	1.29	1.02
16	1.35	0.77	1.08	1.66	1.29	1.04	1.35	1.15	1.54	1.09	2.11	1.07
17	1.81	0.75	1.05	1.92	1.97	1.03	2.33	1.83	1.88	1.40	3.02	1.18
18 *	1.14	1.35	1.28	1.17	0.81	1.00	0.72	0.69	0.95	0.73	1.07	1.02
19	1.00	0.94	1.15	1.59	1.07	0.97	0.96	0.86	1.27	0.90	1.56	1.05
20	1.87	0.73	1.01	1.92	1.76	0.92	1.74	1.48	1.90	1.26	2.47	1.13
21	1.55	0.78	1.21	1.85	1.61	1.09	2.10	1.73	1.52	1.39	2.54	1.12
22	1.40	0.92	1.23	1.56	1.57	1.05	1.29	1.14	1.39	1.08	1.82	1.06
23 *	0.61	0.84	0.54	0.93	0.94	0.84	1.07	1.04	0.87	1.03	1.08	1.00
24	1.11	0.89	0.64	1.27	1.11	0.82	1.14	1.07	1.01	1.07	1.46	0.97
25	1.04	0.84	1.20	1.08	1.14	1.06	1.29	1.22	1.06	1.21	1.25	1.11
26	1.15	0.94	1.35	1.17	1.07	1.18	1.38	1.69	1.12	1.38	1.16	1.20
27	1.21	0.96	1.45	1.92	2.06	1.09	1.21	1.11	1.51	1.22	1.77	1.00
28	1.42	0.77	1.23	1.77	1.65	1.02	1.24	1.16	1.44	1.11	1.48	0.97
29 *	0.76	0.91	1.13	1.05	1.15	1.08	1.34	1.24	1.14	1.13	1.04	1.02
30 *	0.79	0.84	0.64	0.91	0.84	0.76	1.10	0.75	0.82	0.74	0.96	0.86
31	1.16	0.81	1.80	0.88	0.20	0.85	1.27	0.97	0.87	1.11	0.85	1.03
32 *	1.06	0.80	1.72	0.96	0.42	0.89	1.13	1.17	0.88	0.99	0.90	0.93
33	0.58	0.95	0.75	1.01	0.88	1.13	1.43	1.45	1.28	1.29	1.13	1.08
34	4.71	0.84	1.28	2.38	2.86	2.83	1.44	1.25	1.97	1.10	1.51	0.97
35	1.51	0.86	1.54	1.52	1.21	1.29	1.48	1.87	1.90	1.33	1.90	1.22
36	1.35	0.83	1.30	2.69	1.64	1.17	1.51	1.30	2.16	1.21	2.84	1.06
37	2.63	1.21	1.64	2.68	2.38	1.82	0.86	1.27	2.84	1.12	1.48	1.20
38	1.43	0.96	1.40	1.60	1.49	0.97	0.96	0.94	1.23	0.96	1.57	1.03
39	1.29	1.00	1.37	1.48	1.72	1.27	0.94	0.97	1.39	1.10	1.55	1.11
40	1.59	0.99	1.46	2.08	2.29	1.25	1.08	1.34	1.71	1.27	1.78	1.11
41 *	0.56	1.10	1.11	0.95	1.33	1.18	1.15	1.39	1.06	1.32	0.92	1.11
42 *	0.82	0.93	0.89	0.90	1.63	0.98	0.73	0.87	0.87	0.89	0.83	1.01
43 *	0.82	0.98	0.90	0.93	1.26	0.99	0.81	0.87	0.93	0.92	0.83	1.00
44 *	1.13	1.15	0.82	1.12	0.82	1.18	1.25	1.23	1.61	1.14	1.27	1.04
45	1.50	1.13	1.99	2.55	2.44	1.24	1.01	1.19	1.56	1.14	1.78	1.15
Flooded	Mo	Li	As	Pb	Cd	Cu	Cr	Ni	Zn	Co	Ba	V
Average	1.55	0.90	1.26	1.81	1.72	1.16	1.43	1.32	1.56	1.19	1.85	1.08
Stdev	0.75	0.13	0.31	0.55	0.68	0.37	0.50	0.41	0.44	0.26	0.62	0.08
CV	0.48	0.14	0.24	0.30	0.39	0.32	0.35	0.31	0.28	0.22	0.33	0.07
Control	Mo	Li	As	Pb	Cd	Cu	Cr	Ni	Zn	Co	Ba	V
Average	0.99	1.00	0.99	1.00	1.01	1.01	1.01	1.01	1.01	0.99	1.01	1.00
Stdev	0.44	0.18	0.32	0.09	0.34	0.14	0.32	0.33	0.22	0.23	0.14	0.06
CV	0.44	0.18	0.32	0.09	0.34	0.14	0.31	0.32	0.22	0.23	0.14	0.06

* Control samples.

Appendix A.4

Table A4. Contamination factor (CF) of selected elements.

Sample	Mo	Li	As	Pb	Cd	Cu	Cr	Ni	Zn	Co	Ba	V
1	1.52	0.61	0.88	1.75	1.76	0.73	1.48	1.22	1.59	1.00	1.77	0.80
2	1.40	0.68	0.81	1.63	1.10	0.75	1.54	1.37	1.41	1.08	1.95	0.92
3	0.93	0.83	1.42	2.35	2.05	0.86	1.04	0.85	1.28	0.82	1.88	0.86
4	1.19	0.72	1.17	1.74	1.90	1.00	1.94	1.99	1.47	1.60	1.71	0.92
5	1.79	0.74	0.98	1.80	1.90	0.83	1.16	1.05	1.61	0.98	2.01	0.91
6	0.83	0.76	1.25	1.50	1.86	0.85	0.97	0.84	1.05	0.85	1.35	0.83
7	0.83	0.88	0.80	1.11	0.57	0.69	0.90	0.68	0.90	0.61	1.08	0.88
8	1.52	0.55	0.72	1.50	1.33	0.79	2.42	1.78	1.33	1.37	2.25	0.96
9	1.10	0.78	1.14	1.41	1.90	1.00	0.90	0.78	1.23	0.78	1.41	0.86
10 *	2.24	1.23	0.94	1.14	0.71	1.19	0.39	0.41	1.01	0.71	1.23	1.07
11	1.93	1.14	1.34	1.91	2.19	1.35	0.72	0.83	1.73	0.89	1.54	0.97
12	0.36	0.66	0.53	0.50	0.48	0.69	1.51	1.45	0.64	1.32	0.63	0.97
13 *	1.12	0.93	1.01	1.06	1.29	1.04	1.51	1.52	1.06	1.38	1.01	1.06
14	2.00	0.64	0.97	2.16	2.57	1.47	1.33	1.12	1.63	0.99	2.61	0.90
15	1.14	0.84	1.08	1.34	1.29	1.00	1.11	0.92	1.18	0.80	1.21	0.96
16	1.24	0.71	0.99	1.53	1.19	0.96	1.24	1.06	1.42	1.01	1.95	0.99
17	1.36	0.56	0.79	1.44	1.48	0.77	1.75	1.38	1.41	1.05	2.27	0.89
18 *	1.14	1.35	1.28	1.18	0.81	1.01	0.72	0.70	0.95	0.73	1.07	1.02
19	0.93	0.87	1.08	1.48	1.00	0.91	0.89	0.80	1.18	0.84	1.45	0.98
20	1.57	0.61	0.85	1.62	1.48	0.77	1.46	1.24	1.60	1.06	2.08	0.95
21	1.24	0.62	0.97	1.48	1.29	0.87	1.68	1.38	1.22	1.12	2.03	0.90
22	1.19	0.78	1.04	1.32	1.33	0.89	1.10	0.97	1.18	0.92	1.54	0.90
23 *	0.52	0.71	0.46	0.79	0.81	0.72	0.92	0.89	0.75	0.88	0.93	0.86
24	0.90	0.72	0.53	1.04	0.90	0.67	0.94	0.88	0.83	0.87	1.20	0.80
25	0.95	0.76	1.10	0.99	1.05	0.97	1.18	1.12	0.98	1.11	1.15	1.02
26	0.98	0.79	1.15	1.00	0.90	1.00	1.17	1.44	0.95	1.17	0.99	1.02
27	0.95	0.75	1.14	1.51	1.62	0.86	0.96	0.87	1.19	0.96	1.39	0.79
28	1.19	0.64	1.03	1.48	1.38	0.85	1.04	0.97	1.20	0.93	1.24	0.81
29 *	0.69	0.83	1.03	0.95	1.05	0.98	1.22	1.13	1.04	1.04	0.95	0.93
30 *	0.81	0.85	0.65	0.93	0.86	0.78	1.13	0.77	0.84	0.76	0.98	0.88
31	1.12	0.78	1.74	0.86	0.19	0.82	1.23	0.94	0.85	1.07	0.83	1.00
32 *	1.07	0.80	1.74	0.98	0.43	0.90	1.14	1.19	0.89	1.01	0.91	0.94
33	0.50	0.82	0.66	0.88	0.76	0.99	1.25	1.26	1.11	1.13	0.99	0.94
34	3.76	0.67	1.03	1.90	2.29	2.26	1.15	1.00	1.57	0.88	1.21	0.78
35	1.31	0.74	1.34	1.32	1.05	1.12	1.29	1.62	1.65	1.15	1.65	1.06
36	1.10	0.67	1.06	2.18	1.33	0.95	1.23	1.06	1.76	0.98	2.31	0.86
37	2.26	1.03	1.41	2.31	2.05	1.57	0.74	1.09	2.44	0.96	1.28	1.03
38	1.19	0.79	1.17	1.33	1.24	0.81	0.79	0.78	1.02	0.80	1.31	0.86
39	1.14	0.89	1.21	1.31	1.52	1.13	0.83	0.86	1.23	0.98	1.38	0.99
40	1.29	0.80	1.19	1.69	1.86	1.02	0.88	1.09	1.39	1.04	1.44	0.90
41 *	0.50	0.98	1.00	0.85	1.19	1.06	1.03	1.25	0.95	1.18	0.83	1.00
42 *	0.95	1.09	1.04	1.06	1.90	1.15	0.86	1.02	1.02	1.05	0.97	1.18
43 *	0.93	1.11	1.03	1.05	1.43	1.13	0.92	0.98	1.05	1.05	0.94	1.13
44 *	1.05	1.06	0.76	1.04	0.76	1.09	1.16	1.14	1.49	1.06	1.18	0.96
45	1.14	0.86	1.52	1.95	1.86	0.94	0.77	0.91	1.19	0.87	1.36	0.88
Flooded	Mo	Li	As	Pb	Cd	Cu	Cr	Ni	Zn	Co	Ba	V
Average	1.29	0.76	1.06	1.51	1.43	0.97	1.19	1.11	1.31	1.00	1.54	0.91
Stdev	0.59	0.13	0.27	0.43	0.55	0.31	0.37	0.31	0.35	0.19	0.47	0.08
CV	0.46	0.17	0.26	0.28	0.38	0.32	0.31	0.28	0.27	0.19	0.30	0.08
Control	Mo	Li	As	Pb	Cd	Cu	Cr	Ni	Zn	Co	Ba	V
Average	1.00	0.99	0.99	1.00	1.02	1.00	1.00	1.00	1.01	0.99	1.00	1.00
Stdev	0.47	0.19	0.33	0.12	0.41	0.15	0.29	0.30	0.19	0.20	0.12	0.10
CV	0.47	0.19	0.33	0.12	0.40	0.15	0.29	0.30	0.19	0.21	0.12	0.10

* Control samples.

Appendix A.5

Table A5. Correlation matrix for control samples (statistically significant results are marked red, $\alpha = 0.05$).

Parameter	Mo	Cu	Pb	Zn	Ni	Co	Mn	Fe	As	Cd	V	Cr	Ba	Zr	Li	Silt	Sand	Gravel	pH	TC	TIC	TOC	TS	Ca	Al	Mg	Na	K
Mo	1.00																											
Cu	0.53	1.00																										
Pb	0.74	0.67	1.00																									
Zn	0.22	0.61	0.42	1.00																								
Ni	−0.54	−0.01	−0.32	0.25	1.00																							
Co	−0.37	0.24	−0.20	0.33	0.94	1.00																						
Mn	0.13	0.40	−0.01	−0.11	0.28	0.52	1.00																					
Fe	0.11	0.73	0.39	0.27	0.45	0.63	0.58	1.00																				
As	0.20	0.26	0.40	−0.03	0.20	0.13	−0.08	0.49	1.00																			
Cd	−0.24	0.45	0.08	0.10	0.28	0.46	0.51	0.68	−0.15	1.00																		
V	0.39	0.85	0.64	0.28	0.01	0.25	0.47	0.85	0.28	0.71	1.00																	
Cr	−0.57	−0.31	−0.37	0.18	0.88	0.74	0.04	0.10	0.03	0.09	−0.30	1.00																
Ba	0.80	0.40	0.68	0.54	−0.51	−0.41	−0.16	−0.18	−0.16	−0.30	0.15	−0.42	1.00															
Zr	0.84	0.45	0.60	−0.01	−0.77	−0.61	−0.03	0.06	0.10	−0.06	0.47	−0.82	0.60	1.00														
Li	0.58	0.73	0.84	0.37	−0.46	−0.30	0.01	0.31	0.20	0.17	0.65	−0.62	0.57	0.61	1.00													
Silt	−0.11	−0.22	0.09	−0.32	−0.10	−0.23	−0.28	−0.01	0.45	−0.18	−0.03	−0.25	−0.15	−0.05	0.14	1.00												
Sand	0.20	0.36	0.15	0.18	0.01	0.10	0.06	0.20	0.06	0.24	0.29	0.07	0.02	0.31	0.14	−0.71	1.00											
Gravel	−0.14	−0.24	−0.32	0.14	0.11	0.14	0.26	−0.27	−0.63	−0.11	−0.37	0.20	0.16	−0.37	−0.36	−0.23	−0.52	1.00										
pH	0.03	0.03	−0.12	0.01	0.04	0.19	0.58	−0.08	−0.63	0.18	0.02	−0.04	0.19	−0.15	0.05	−0.09	−0.36	0.61	1.00									
TC	−0.39	0.13	0.03	0.25	0.32	0.21	−0.43	0.30	0.40	0.32	0.22	0.18	−0.29	−0.20	0.07	0.40	0.05	−0.56	−0.50	1.00								
TIC	0.00	0.38	0.19	0.69	0.14	0.16	−0.27	0.17	−0.15	0.34	0.30	0.03	0.33	0.05	0.20	0.01	0.05	−0.08	−0.02	0.64	1.00							
TOC	−0.47	0.00	−0.04	0.02	0.34	0.18	−0.42	0.29	0.54	0.25	0.15	0.20	−0.49	−0.26	0.00	0.49	0.04	−0.65	−0.60	0.95	0.37	1.00						
TS	−0.30	0.07	0.11	0.28	0.24	0.07	−0.60	0.16	0.51	0.05	0.08	0.14	−0.18	−0.19	0.12	0.50	−0.04	−0.56	−0.59	0.95	0.55	0.93	1.00					
Ca	−0.17	0.20	−0.02	0.86	0.48	0.43	−0.23	0.03	−0.14	−0.05	−0.14	0.49	0.26	−0.41	−0.10	−0.27	−0.01	0.35	−0.01	0.29	0.63	0.10	0.34	1.00				
Al	0.51	0.77	0.55	0.09	−0.30	−0.02	0.55	0.66	0.13	0.54	0.87	−0.62	0.26	0.61	0.66	0.09	0.02	−0.14	0.20	−0.05	0.14	−0.12	−0.16	−0.31	1.00			
Mg	−0.33	0.14	−0.21	0.43	0.89	0.93	0.47	0.43	−0.07	0.32	0.07	0.77	−0.21	−0.66	−0.37	−0.26	−0.09	0.44	0.36	0.06	0.23	−0.02	−0.05	0.59	−0.12	1.00		
Na	−0.60	−0.61	−0.77	−0.32	0.39	0.34	0.20	−0.25	−0.56	0.11	−0.42	0.44	−0.45	−0.57	−0.76	−0.01	−0.40	0.57	0.48	−0.15	−0.04	−0.16	−0.29	0.04	−0.36	0.46	1.00	
K	0.37	0.39	0.04	0.12	−0.47	−0.22	0.41	−0.04	−0.59	0.17	0.26	−0.63	0.42	0.46	0.35	−0.25	−0.03	0.34	0.63	−0.43	0.15	−0.59	−0.52	−0.09	0.57	−0.14	0.05	1.00

Appendix A.6

Table A6. Correlation matrix for flooded samples (statistically significant results are marked red, $\alpha = 0.05$).

Parameter	Mo	Cu	Pb	Zn	Ni	Co	Mn	Fe	As	Cd	V	Cr	Ba	Zr	Li	Silt	Sand	Gravel	pH	TC	TIC	TOC	TS	Ca	Al	Mg	Na	K
Mo	1.00																											
Cu	0.81	1.00																										
Pb	0.56	0.43	1.00																									
Zn	0.64	0.52	0.79	1.00																								
Ni	0.02	−0.06	−0.09	0.17	1.00																							
Co	−0.09	−0.08	−0.19	0.04	0.92	1.00																						
Mn	0.09	0.11	0.21	0.23	0.42	0.52	1.00																					
Fe	0.31	0.24	0.21	0.50	0.70	0.62	0.64	1.00																				
As	0.14	0.28	0.34	0.22	−0.27	−0.18	0.28	0.09	1.00																			
Cd	0.61	0.55	0.82	0.64	−0.09	−0.14	0.27	0.15	0.26	1.00																		
V	−0.14	0.04	−0.26	0.11	0.34	0.38	0.32	0.62	0.23	−0.34	1.00																	
Cr	0.02	−0.22	−0.10	0.02	0.84	0.76	0.26	0.55	−0.44	−0.13	0.11	1.00																
Ba	0.27	−0.02	0.62	0.54	0.28	0.14	0.39	0.50	−0.14	0.47	−0.11	0.46	1.00															
Zr	−0.28	0.11	−0.32	−0.20	−0.29	−0.12	−0.07	−0.13	0.35	−0.39	0.54	−0.50	−0.63	1.00														
Li	−0.02	0.26	0.12	0.14	−0.49	−0.41	−0.10	−0.25	0.52	0.11	0.31	−0.73	−0.44	0.66	1.00													
Silt	0.21	0.30	0.21	0.21	−0.05	0.09	0.03	−0.08	0.40	0.27	0.02	−0.26	−0.19	0.15	0.29	1.00												
Sand	−0.33	−0.38	−0.27	−0.41	−0.09	−0.12	0.00	0.08	−0.22	−0.34	0.12	0.15	0.17	−0.08	−0.31	−0.58	1.00											
Gravel	0.27	0.27	0.20	0.37	0.14	0.09	−0.02	−0.05	0.02	0.25	−0.16	−0.03	−0.09	0.01	0.20	0.09	−0.87	1.00										
pH	0.14	−0.01	0.13	−0.08	−0.22	−0.26	0.23	0.14	0.03	0.24	−0.11	−0.09	0.36	−0.28	−0.24	−0.08	0.32	−0.34	1.00									
TC	0.32	0.17	0.38	0.36	0.46	0.43	0.19	0.30	0.05	0.24	−0.15	0.40	0.28	−0.31	−0.32	0.22	−0.44	0.40	−0.13	1.00								
TIC	0.04	−0.27	0.23	0.12	0.26	0.23	0.11	−0.03	−0.14	0.16	−0.38	0.30	0.28	−0.51	−0.35	0.05	−0.32	0.35	−0.05	0.65	1.00							
TOC	0.39	0.42	0.33	0.38	0.41	0.40	0.17	0.41	0.17	0.20	0.08	0.30	0.16	−0.03	−0.17	0.25	−0.34	0.27	−0.13	0.83	0.12	1.00						
TS	0.29	0.27	0.15	0.34	0.12	0.08	0.22	0.44	0.15	−0.01	0.29	0.06	0.25	0.09	−0.10	−0.11	0.13	−0.08	0.13	0.28	−0.23	0.54	1.00					
Ca	0.32	−0.09	0.44	0.43	0.33	0.19	0.22	0.32	−0.35	0.36	−0.28	0.53	0.77	−0.77	−0.58	−0.20	−0.01	0.14	0.30	0.37	0.51	0.11	0.06	1.00				
Al	−0.23	0.19	−0.22	−0.10	−0.23	−0.13	0.06	−0.04	0.40	−0.17	0.52	−0.60	−0.58	0.84	0.75	0.19	−0.16	0.08	−0.17	−0.31	−0.47	−0.06	0.07	−0.81	1.00			
Mg	0.07	−0.28	0.16	0.23	0.69	0.58	0.28	0.49	−0.50	0.09	−0.01	0.85	0.69	−0.66	−0.69	−0.24	0.17	−0.06	0.12	0.36	0.41	0.17	0.05	0.83	−0.73	1.00		
Na	−0.50	−0.35	−0.65	−0.67	−0.10	0.02	−0.31	−0.48	−0.51	−0.56	−0.04	−0.07	−0.50	0.32	−0.03	−0.12	0.15	−0.11	−0.11	−0.35	−0.11	−0.38	−0.33	−0.34	0.21	−0.12	1.00	
K	−0.32	0.06	−0.22	−0.24	−0.48	−0.36	0.01	−0.27	0.28	−0.12	0.24	−0.73	−0.50	0.69	0.68	0.05	−0.03	0.01	0.00	−0.47	−0.43	−0.30	0.02	−0.71	0.87	−0.76	0.33	1.00

Appendix A.7

Table A7. Average values, standard deviations, and coefficients of variation (Cv).

Parameter	Flooded Samples			Control Samples		
	Average	Standard Deviation	Cv	Average	Standard Deviation	Cv
Mo	0.54	0.25	0.45	0.42	0.20	0.47
Cu	46.78	14.69	0.31	48.21	7.27	0.15
Pb	43.82	12.29	0.28	29.07	3.35	0.12
Zn	120.20	31.48	0.26	92.46	17.39	0.19
Ni	280.90	76.84	0.27	253.92	76.92	0.30
Co	31.00	5.79	0.19	30.55	6.34	0.21
Mn	1245.59	162.76	0.13	1232.36	300.78	0.24
Fe	3.89	0.41	0.11	3.85	0.41	0.11
As	16.97	4.29	0.25	15.89	5.31	0.33
Cd	0.30	0.11	0.38	0.21	0.09	0.40
V	90.44	7.50	0.08	99.27	10.11	0.10
Cr	471.53	145.76	0.31	395.09	115.28	0.29
Ba	407.15	122.35	0.30	264.36	31.45	0.12
Zr	52.37	7.15	0.14	67.29	7.76	0.12
Li	36.25	5.96	0.16	47.65	9.28	0.19
Silt	9.54	2.93	0.31	11.56	3.88	0.34
Sand	85.63	5.81	0.07	82.21	4.44	0.05
Gravel	4.84	4.77	0.99	6.23	3.20	0.51
pH	7.14	0.25	0.03	7.11	0.24	0.03
TC	2.72	0.94	0.35	2.71	0.94	0.35
TIC	0.47	0.52	1.12	0.14	0.32	2.23
TOC	2.25	0.72	0.32	2.57	0.78	0.30
TS	0.03	0.02	0.64	0.04	0.01	0.33
Ca	2.31	1.26	0.55	0.92	0.64	0.70
Al	5.26	0.50	0.10	5.96	0.42	0.07
Mg	2.36	0.97	0.41	1.64	0.54	0.33
Na	0.84	0.18	0.21	0.93	0.23	0.25
K	1.20	0.16	0.13	1.38	0.21	0.15

Appendix A.8

Table A8. Eigenvalues for flooded samples.

Value	Eigenvalues for Flooded Samples Extraction: Principal Components		
	Eigenvalue	Total (%)	Cumulative (%)
1	8.14	29.06	29.06
2	5.35	19.12	48.18
3	3.70	13.23	61.40
4	2.90	10.36	71.76
5	1.52	5.42	77.17

Appendix A.9

Table A9. Factor loadings for flooded samples using Varimax raw rotation.

Variable	Factor Loadings for Flooded Samples (Varimax Raw) Extraction: Principal Components (Marked Loadings Are >0.7)				
	Factor 1	**Factor 2**	**Factor 3**	**Factor 4**	**Factor 5**
Mo	0.157	0.591	−0.111	0.168	0.579
Cu	−0.259	0.475	−0.077	0.190	0.627
Pb	0.161	0.876	−0.096	0.162	0.114
Zn	0.069	0.758	0.183	0.232	0.306
Ni	0.385	−0.137	0.831	0.211	0.098
Co	0.238	−0.199	0.867	0.255	0.016
Mn	−0.046	0.432	0.688	−0.102	−0.193
Fe	0.104	0.348	0.837	−0.185	0.255
As	−0.579	0.496	0.057	0.075	0.009
Cd	0.122	0.854	−0.149	0.190	0.030
V	−0.500	−0.078	0.701	−0.233	0.097
Cr	0.698	−0.195	0.617	0.017	0.091
Ba	0.603	0.596	0.253	−0.250	−0.029
Zr	−0.867	−0.289	0.064	0.005	0.096
Li	−0.838	0.203	−0.198	0.161	−0.107
Silt	−0.296	0.252	−0.003	0.484	0.016
Sand	0.168	−0.240	0.018	−0.894	−0.060
Gravel	−0.023	0.138	−0.020	0.793	0.064
pH	0.173	0.359	−0.117	−0.545	−0.108
TC	0.390	0.188	0.299	0.583	0.356
TIC	0.547	0.117	0.059	0.533	−0.316
TOC	0.112	0.161	0.349	0.374	0.696
TS	−0.057	0.172	0.266	−0.278	0.696
Ca	0.821	0.396	0.130	0.002	−0.068
Al	−0.943	−0.099	0.095	0.029	−0.006
Mg	0.818	0.065	0.479	−0.058	−0.076
Na	−0.100	−0.756	−0.171	−0.017	−0.246
K	−0.836	−0.083	−0.168	−0.116	−0.178

Appendix A.10

Table A10. Eigenvalues for control samples.

Value	Eigenvalues for Control Samples Extraction: Principal Components		
	Eigenvalue	**Total (%)**	**Cumulative (%)**
1	7.72	27.57	27.57
2	6.13	21.88	49.45
3	5.26	18.79	68.23
4	3.25	11.59	79.83
5	2.22	7.95	87.77
6	1.76	6.28	94.06

Appendix A.11

Table A11. Factor loadings for control samples using Varimax raw rotation.

Variable	Factor Loadings for Control Samples (Varimax Raw) Extraction: Principal Components (Marked Loadings Are >0.7)					
	Factor 1	**Factor 2**	**Factor 3**	**Factor 4**	**Factor 5**	**Factor 6**
Mo	0.310	−0.416	−0.560	0.306	−0.084	0.463
Cu	0.821	−0.010	−0.096	0.439	−0.194	0.202
Pb	0.489	−0.016	−0.390	0.415	0.029	0.558
Zn	0.187	0.075	0.183	0.937	−0.147	0.060
Ni	0.066	0.170	0.972	0.051	−0.015	0.044
Co	0.334	0.016	0.922	0.089	−0.081	−0.016
Mn	0.658	−0.563	0.361	−0.264	−0.019	−0.095
Fe	0.860	0.156	0.375	−0.009	−0.058	0.249
As	0.202	0.412	0.085	−0.164	0.105	0.840
Cd	0.746	0.218	0.256	−0.100	−0.190	−0.419
V	0.956	0.120	−0.088	0.093	−0.116	0.107
Cr	−0.301	0.086	0.902	0.066	−0.155	0.051
Ba	0.054	−0.357	−0.521	0.722	0.032	0.172
Zr	0.354	−0.141	−0.823	0.065	−0.205	0.195
Li	0.574	0.050	−0.552	0.345	0.060	0.257
Silt	−0.001	0.436	−0.175	−0.220	0.826	0.187
Sand	0.170	0.087	−0.056	0.015	−0.960	0.122
Gravel	−0.233	−0.649	0.289	0.245	0.329	−0.395
pH	0.216	−0.628	0.126	0.095	0.347	−0.496
TC	0.126	0.963	0.145	0.156	0.052	−0.031
TIC	0.214	0.488	0.008	0.711	0.000	−0.359
TOC	0.066	0.968	0.173	−0.099	0.063	0.108
TS	−0.042	0.941	0.060	0.231	0.142	0.165
Ca	−0.181	0.131	0.449	0.838	−0.046	−0.088
Al	0.911	−0.125	−0.330	0.001	0.118	−0.001
Mg	0.169	−0.161	0.918	0.284	0.056	−0.100
Na	−0.282	−0.194	0.485	−0.264	0.240	−0.643
K	0.386	−0.489	−0.430	0.185	0.029	−0.537

References

1. Vácha, R.; Sáňka, M.; Sáňka, O.; Skála, J.; Čechmánková, J. The Fluvisol and Sediment Trace Element Contamination Level as Related to Their Geogenic and Anthropogenic Source. *Plant Soil Environ.* **2013**, *59*, 136–142. [CrossRef]
2. Martynov, A.V. Influence of the Large Flood on the Element Composition of Fluvisols in the Amur River Valley. *Geogr. Environ. Sustain.* **2020**, *13*, 52–64. [CrossRef]
3. Ružičić, S.; Balaž, B.-I.; Kovač, Z.; Filipović, L.; Nakić, Z.; Kopić, J. Nickel and Chromium Origin in Fluvisols of the Petruševec Well Field, Zagreb Aquifer. *Environments* **2022**, *9*, 154. [CrossRef]
4. Förstner, U.; Heise, S.; Schwartz, R.; Westrich, B.; Ahlf, W. Historical Contaminated Sediments and Soils at the River Basin Scale. *J. Soils Sediments* **2004**, *4*, 247–260. [CrossRef]

5. Lair, G.J.; Zehetner, F.; Fiebig, M.; Gerzabek, M.H.; van Gestel, C.A.M.; Hein, T.; Hohensinner, S.; Hsu, P.; Jones, K.C.; Jordan, G.; et al. How Do Long-Term Development and Periodical Changes of River–Floodplain Systems Affect the Fate of Contaminants? Results from European Rivers. *Environ. Pollut.* **2009**, *157*, 3336–3346. [CrossRef] [PubMed]
6. Krami, L.K.; Amiri, F.; Sefiyanian, A.; Shariff, A.R.B.M.; Tabatabaie, T.; Pradhan, B. Spatial Patterns of Heavy Metals in Soil under Different Geological Structures and Land Uses for Assessing Metal Enrichments. *Environ. Monit. Assess.* **2013**, *185*, 9871–9888. [CrossRef]
7. Arias-Navarro, C.; Vidojević, D.; Zdruli, P.; Yunta Mezquita, F.; Jones, A.; Wojda, P. Addressing Point Source Soil Pollution in the Western Balkans: Challenges and Opportunities for European Union Integration. *Integr. Environ. Assess. Manag.* **2025**, vjaf104. [CrossRef]
8. Šapčanin, A.; Bikić, F. The Long-Term Impact of Heavy Metals from the Bosna River on Human Health. In *Proceedings of the 14th Scientific/Research Symposium with International Participation „Metallic and Nonmetallic Materials", Zenica, Bosnia and Herzegovina, 27–28 April 2023*; Bikić, F., Ed.; University of Zenica Faculty of Metallurgy and Technology: Zenica, Bosnia and Herzegovina, 2023; pp. 280–285.
9. Karahmet, E.; Isaković, S.; Bečić, E.; Bečić, F.; Smailović, A. Monitoring the Bosna and Krivaja Rivers Pollution by Heavy Metals (In Croatian: Monitoring Onečišćenja Teškim Metalima Rijeka Krivaje i Bosne). *Hrvat. Vode* **2023**, *31*, 259–264.
10. Barbieri, M. The Importance of Enrichment Factor (EF) and Geoaccumulation Index (Igeo) to Evaluate the Soil Contamination. *J. Geol. Geophys.* **2016**, *5*, 1000237. [CrossRef]
11. Baghel, C.; Tiwari, A.; Bachkaiya, V. Study of Correlation between Soil Chemical Properties, Zinc Fractions and Yield of Rice under Long Term Fertilization in Chromustert Soil. *Int. J. Plant Soil Sci.* **2023**, *35*, 351–358. [CrossRef]
12. Ghavamifar, S.; Golsefidi, H.T.; Samani, A.B.; Li, Z.; Naidu, R. The Correlation of Soil Properties, Climate Factors, and ^{137}Cs Activity in Soils. *Soil Sci. Soc. Am. J.* **2025**, *89*, e70122. [CrossRef]
13. Maione, C.; Luíza da Costa, N.; Barbosa, F.; Barbosa, R.M. A Cluster Analysis Methodology for the Categorization of Soil Samples for Forensic Sciences Based on Elemental Fingerprint. *Appl. Artif. Intell.* **2022**, *36*, e2010941. [CrossRef]
14. Vinay, H.T.; Mallikarjun, B.H.; Jagadeesh, M.S.; Ramamurthy, V.; Mohan Kumar, T.L.; Krishnamurthy, K. Clustering Approach to Group Similar Soils for Efficient Agricultural Land Use Planning. *Int. J. Stat. Appl. Math.* **2024**, *9*, 61–68. [CrossRef]
15. Zhu, F.; Zhu, C.; Fang, Z.; Lu, W.; Pan, J. Using Constrained K-Means Clustering for Soil Texture Mapping with Limited Soil Samples. *Agronomy* **2025**, *15*, 1220. [CrossRef]
16. Martín-Sanz, J.P.; de Santiago-Martín, A.; Valverde-Asenjo, I.; Quintana-Nieto, J.R.; González-Huecas, C.; López-Lafuente, A.L. Comparison of Soil Quality Indexes Calculated by Network and Principal Component Analysis for Carbonated Soils under Different Uses. *Ecol. Indic.* **2022**, *143*, 109374. [CrossRef]
17. Menge, D.M.; Musila, R.N.; Kagito, S.; Bii, L.; Gichuki, J.; Gichuhi, E.; Kundu, C.A.; Murori, R.; Ismail, A.; Panchbhai, A. Using Principal Component Analysis to Assess Soil Chemical Properties in the Mwea Irrigation Scheme, Kenya: Implications for Rice Agronomic Management. *Int. J. Plant Soil Sci.* **2024**, *36*, 106–126. [CrossRef]
18. Shokr, M.S.; Jalhoum, M.E.M.; Sayed, A.S.A.; Saeed, M.; Rebouh, N.Y.; Mohamed, E.S.; Yousif, I.A.H.; Abdelhameed, H.H. Assessment of Soil Quality in Arid Zones Using Principal Component Analysis and GIS-Based Modeling. *PLoS ONE* **2025**, *20*, e0337063. [CrossRef]
19. Bünemann, E.K.; Bongiorno, G.; Bai, Z.; Creamer, R.E.; De Deyn, G.; de Goede, R.; Fleskens, L.; Geissen, V.; Kuyper, T.W.; Mäder, P.; et al. Soil Quality—A Critical Review. *Soil Biol. Biochem.* **2018**, *120*, 105–125. [CrossRef]
20. Hamidi Nehrani, S.; Askari, M.S.; Saadat, S.; Delavar, M.A.; Taheri, M.; Holden, N.M. Quantification of Soil Quality under Semi-Arid Agriculture in the Northwest of Iran. *Ecol. Indic.* **2020**, *108*, 105770. [CrossRef]
21. Shi, Y.; Xu, X.; Li, Q.; Zhang, M.; Li, J.; Lu, Y.; Liang, R.; Zheng, X.; Shao, X. Integrated Regional Ecological Risk Assessment of Multiple Metals in the Soils: A Case in the Region around the Bohai Sea and the Yellow Sea. *Environ. Pollut.* **2018**, *242*, 288–297. [CrossRef] [PubMed]
22. Monaci, F.; Baroni, D. Spatial Distribution and Ecological Risk of Potentially Toxic Elements in Peri-Urban Soils of a Historically Industrialised Area. *Environ. Monit. Assess.* **2025**, *197*, 948. [CrossRef] [PubMed]
23. Pamić, J.; Sunarić-Pamić, O.; Kapelar, I.; Olujić, J. *Explanation of the Basic Geological Map—Sheet Zavidovići L34-121*; Federal Geological Institute: Belgrade, Serbia, 1973.
24. Salkić, Z. Petrology and Gechemistry of the Tartiary Vulcanics in Bosina and Herzegovina (In Bosnian: Petrologija i Geohemija Tercijarnih Vulkanskih Stijena u Bosni i Hercegovini). Ph.D. Thesis, Faculty of Mining, Geology and Civil Engineering, University of Tuzla, Tuzla, Bosnia and Herzegovina, 2005.
25. Laušević, M.; Jovanović, Č. *The Basic Geological Map of the Former SFR Yugoslavia 1:100,000, Geological Sheet Doboj; Sarajevo*; Federal Geological Institute: Belgrade, Serbia, 1982.
26. Varol, M.; Sünbül, M.R.; Aytop, H.; Yılmaz, C.H. Environmental, Ecological and Health Risks of Trace Elements, and Their Sources in Soils of Harran Plain, Turkey. *Chemosphere* **2020**, *245*, 125592. [CrossRef] [PubMed]

27. Dali-Youcef, N.; Ouddane, B.; Derriche, Z. Metal Found in Superficial Sediments of the Tafna River and Its Estuary in North-Western Algeria. *Fresenius Environ. Bull.* **2005**, *14*, 753–763.
28. Boës, X.; Rydberg, J.; Martinez-Cortizas, A.; Bindler, R.; Renberg, I. Evaluation of Conservative Lithogenic Elements (Ti, Zr, Al, and Rb) to Study Anthropogenic Element Enrichments in Lake Sediments. *J. Paleolimnol.* **2011**, *46*, 75–87. [CrossRef]
29. Brenko, T.; Borojević Šoštarić, S.; Ružičić, S.; Sekelj Ivančan, T. Evidence for the Formation of Bog Iron Ore in Soils of the Podravina Region, NE Croatia: Geochemical and Mineralogical Study. *Quat. Int.* **2020**, *536*, 13–29. [CrossRef]
30. Birch, G.A. Scheme for Assessing Human Impacts on Coastal Aquatic Environments Using Sediments. In *Coastal GIS 2003: An Integrated Approach to Australian Coastal Issues*; Woodroffe, C.D., Furness, R.A., Eds.; Centre for Maritime Policy, University of Wollongong: Wollongong, Australia, 2003; p. 553. ISBN 1741280230.
31. Rajmohan, N.; Prathapar, S.A.; Jayaprakash, M.; Nagarajan, R. Vertical Distribution of Heavy Metals in Soil Profile in a Seasonally Waterlogging Agriculture Field in Eastern Ganges Basin. *Environ. Monit. Assess.* **2014**, *186*, 5411–5427. [CrossRef]
32. Pekey, H.; Karakaş, D.; Ayberk, S.; Tolun, L.; Bakoğlu, M. Ecological Risk Assessment Using Trace Elements from Surface Sediments of İzmit Bay (Northeastern Marmara Sea) Turkey. *Mar. Pollut. Bull.* **2004**, *48*, 946–953. [CrossRef]
33. Wójcik-Leń, J. An Algorithm for Delimiting Rural Areas According to Soil Classes. *Land* **2022**, *11*, 158. [CrossRef]
34. Bougiouklis, J.-N.; Barouchas, P.E.; Petropoulos, P.; Tsesmelis, D.E.; Moustakas, N. Precision Soil Sampling Strategy for the Delineation of Management Zones in Olive Cultivation Using Unsupervised Machine Learning Methods. *Sci. Rep.* **2025**, *15*, 8253. [CrossRef]
35. Sanad, H.; Moussadek, R.; Zouahri, A.; Oueld Lhaj, M.; Dakak, H.; Manhou, K.; Mouhir, L. Heavy Metal-Induced Variability in Leaf Nutrient Uptake and Photosynthetic Traits of Avocado (*Persea Americana*) in Mediterranean Soils: A Multivariate and Probabilistic Modeling of Soil-to-Plant Transfer Risks. *Plants* **2026**, *15*, 205. [CrossRef]
36. Jakab, G.; Madarász, B.; Masoudi, M.; Karlik, M.; Király, C.; Zacháry, D.; Filep, T.; Dekemati, I.; Centeri, C.; Al-Graiti, T.; et al. Soil Organic Matter Gain by Reduced Tillage Intensity: Storage, Pools, and Chemical Composition. *Soil Tillage Res.* **2023**, *226*, 105584. [CrossRef]
37. Tomaz, A.; Martins, I.; Catarino, A.; Mourinha, C.; Dôres, J.; Fabião, M.; Boteta, L.; Coutinho, J.; Patanita, M.; Palma, P. Insights into the Spatial and Temporal Variability of Soil Attributes in Irrigated Farm Fields and Correlations with Management Practices: A Multivariate Statistical Approach. *Water* **2022**, *14*, 3216. [CrossRef]
38. Yuan, Y.; Luo, Y.; Wang, H.; Ren, Y.; Mei, N.; Zheng, H.; Liu, W.; Liang, A.; Chen, X.; Zhang, Y.; et al. A Comparative Analysis of Soil Health Index Calculation Methods and Minimum Dataset Construction Approaches: A Case Study from a 40-Year Tillage Experiment. *Ecol. Indic.* **2026**, *182*, 114609. [CrossRef]
39. Baghbani, A.; Bahrampour, D.; Moballegh, A.; Daghistani, F. A Curated Experimental Dataset of UCS and CBR Results from Biopolymer-Based Two-Additive Stabilisation Studies on Fine-Grained Soils. *Data* **2026**, *11*, 109. [CrossRef]
40. Wu, Y.; Wang, Y.; Yang, W.; Zhang, J.; Wu, Y.; Li, J.; Zhang, G.; Bing, H. Multi-Element Dataset of Soil Profiles across Climatic Zones in China's Mountains. *Earth Syst. Sci. Data* **2025**, *17*, 4779–4797. [CrossRef]
41. Arroyo-Cruz, C.E.; Prado, B.; Kolb, M.; Mora-Palomino, L.N.; Todd-Brown, K.; Guevara, M. Synthesis of a National Soil Dataset Across Productive Land in Mexico: The Importance of Making Existing Data Accessible. *Eur. J. Soil Sci.* **2025**, *76*, e70116. [CrossRef]
42. Barrena-González, J.; Lavado Contador, J.F.; Pulido Fernández, M. Mapping Soil Properties at a Regional Scale: Assessing Deterministic vs. Geostatistical Interpolation Methods at Different Soil Depths. *Sustainability* **2022**, *14*, 10049. [CrossRef]
43. Federation BiH. *n.d. No. 96/22 Rulebook on Determination of Permitted Amounts of Harmful and Dangerous Substances in the Soil and Their Testing Methods*; Službene novine Federacije BiH: Sarajevo, Bosnia and Herzegovina, 2022.
44. Mandal, B.K.; Suzuki, K.T. Arsenic Round the World: A Review. *Talanta* **2002**, *58*, 201–235. [CrossRef]
45. Halamić, J.; Miko, S. *Geokemijski Atlas Republike Hrvatske = Geochemical Atlas of the Republic of Croatia*; Halamić, J., Slobodan, M., Eds.; Hrvatski Geološki Institut = Croatian Geological Survey: Zagreb, Croatia, 2009; ISBN 9789536907182.
46. Predić, T.; Nikić Nauth, P.; Radanović, B.; Predić, A. State of Heavy Metals Pollution of Flooded Agricultural Land in the North Part of Republic of Srpska. *Agro Knowl. J.* **2017**, *17*, 19. [CrossRef]
47. Ximenes, M.; Pratas, J.A.M.S.; De Azevedo, J.M.M.; Ribeiro, J. Evaluating the Concentration, Distribution, and Contamination of Toxic Metals in the Urban Soil of Dili, Timor-Leste. *Geol. Ecol. Landsc.* **2025**, 1–22. [CrossRef]
48. Babajić, E.; Babajić, A.; Stjepić Srkalović, Ž.; Srkalović, D.; Ustalić, S.; Akmadžić, H. Chromium and Nickel in Soil in the Wider Maglaj Area—Concentration and Genesis. *Arch. Tech. Sci.* **2017**, *2*, 13–20. [CrossRef]
49. Kobierski, M. Evaluation of the Content of Heavy Metals in Fluvisols of Floodplain Area Depending on the Type of Land Use. *J. Ecol. Eng.* **2015**, *16*, 23–31. [CrossRef]
50. Bayraklı, B.; Dengiz, O. Determination of Heavy Metal Risk and Their Enrichment Factor in Intensive Cultivated Soils of Tokat Province. *Eurasian J. Soil Sci.* **2019**, *8*, 249–256. [CrossRef]
51. Steingräber, L.F.; Ludolphy, C.; Metz, J.; Germershausen, L.; Kierdorf, H.; Kierdorf, U. Heavy Metal Concentrations in Floodplain Soils of the Innerste River and in Leaves of Wild Blackberries (*Rubus Fruticosus* L. Agg.) Growing within and Outside the

Floodplain: The Legacy of Historical Mining Activities in the Harz Mountains (Germany). *Environ. Sci. Pollut. Res.* **2022**, *29*, 22469–22482. [CrossRef]
52. Kabata-Pendias, A. *Trace Elements in Soils and Plants*, 4th ed.; CRC Press: Boca Raton, FL, USA, 2010; ISBN 9780429192036.
53. Cappuyns, V.; Slabbinck, E. Occurrence of Vanadium in Belgian and European Alluvial Soils. *Appl. Environ. Soil Sci.* **2012**, *2012*, 979501. [CrossRef]
54. Zhou, W.; Han, G.; Liu, M.; Song, C.; Li, X.; Malem, F. Vertical Distribution and Controlling Factors Exploration of Sc, V, Co, Ni, Mo and Ba in Six Soil Profiles of The Mun River Basin, Northeast Thailand. *Int. J. Environ. Res. Public Health* **2020**, *17*, 1745. [CrossRef]
55. Ilić, P.; Ilić, S.; Nešković Markić, D.; Stojanović Bjelić, L.; Popović, Z.; Radović, B.; Mrazovac Kurilić, S.; Farooqi, Z.U.R.; Mehmood, T.; Mohamed, M.H.; et al. Ecological Risk of Toxic Metal Contamination in Soil around Coal Mine and Thermal Power Plant. *Pol. J. Environ. Stud.* **2022**, *31*, 4147–4156. [CrossRef]
56. Kanianska, R.; Drimal, M.; Varga, J.; Komárek, M.; Ahado, S.K.; Šťastná, M.; Kizeková, M.; Jančová, Ľ. Critically Raw Materials as Potential Emerging Environmental Contaminants, Their Distribution Patterns, Risks and Behaviour in Floodplain Soils Contaminated by Heavy Metals. *Sci. Rep.* **2023**, *13*, 9597. [CrossRef] [PubMed]
57. Tomczyk, P.; Wdowczyk, A.; Wiatkowska, B.; Szymańska-Pulikowska, A. Assessment of Heavy Metal Contamination of Agricultural Soils in Poland Using Contamination Indicators. *Ecol. Indic.* **2023**, *156*, 111161. [CrossRef]
58. Miko, S.; Halamić, J.; Peh, Z.; Galović, L. Geochemical Baseline Mapping of Soils Developed on Diverse Bedrock from Two Regions in Croatia. *Geol. Croat.* **2001**, *54*, 53–118. [CrossRef]
59. Aliu, M.; Šajn, R.; Stafilov, T. Occurrence and Enrichment Sources of Cobalt, Chromium, and Nickel in Soils of Mitrovica Region, Republic of Kosovo. *J. Environ. Sci. Health Part A* **2021**, *56*, 566–571. [CrossRef]
60. Kanianska, R.; Varga, J.; Benková, N.; Kizeková, M.; Jančová, Ľ. Floodplain Soils Contamination Assessment Using the Sequential Extraction Method of Heavy Metals from Past Mining Activities. *Sci. Rep.* **2022**, *12*, 2927. [CrossRef] [PubMed]
61. Wang, Y.; Chen, F.; Zhang, M.; Chen, S.; Tan, X.; Liu, M.; Hu, Z. The Effects of the Reverse Seasonal Flooding on Soil Texture within the Hydro-Fluctuation Belt in the Three Gorges Reservoir, China. *J. Soils Sediments* **2018**, *18*, 109–115. [CrossRef]
62. Yang, Z.; Carling, P.A.; Liu, W.; Zhou, G.G.D.; Wang, H.; Yang, A. Saturated, Smashed, and Suppressed: The Fate of Suspended Gravel in Large Palaeofloods. *J. Geophys. Res. Earth Surf.* **2026**, *131*, e2025JF008632. [CrossRef]
63. Baldwin, D.S.; Paul, W.L.; Wilson, J.S.; Pitman, T.; Rees, G.N.; Klein, A.R. Changes in Soil Carbon in Response to Flooding of the Floodplain of a Semi-Arid Lowland River. *Freshw. Sci.* **2015**, *34*, 431–439. [CrossRef]
64. Adamczyk-Szabela, D.; Wolf, W.M. The Impact of Soil PH on Heavy Metals Uptake and Photosynthesis Efficiency in *Melissa officinalis*, *Taraxacum officinalis*, *Ocimum basilicum*. *Molecules* **2022**, *27*, 4671. [CrossRef] [PubMed]
65. Kicińska, A.; Pomykała, R.; Izquierdo-Diaz, M. Changes in Soil pH and Mobility of Heavy Metals in Contaminated Soils. *Eur. J. Soil Sci.* **2022**, *73*, e13203. [CrossRef]
66. Ollson, C.J.; Smith, E.; Scheckel, K.G.; Betts, A.R.; Juhasz, A.L. Assessment of Arsenic Speciation and Bioaccessibility in Mine-Impacted Materials. *J. Hazard. Mater.* **2016**, *313*, 130–137. [CrossRef]
67. Irwin, C.; Gudka, S.; De Meyer, S.; Dennekamp, M.; Netherway, P.; Moslehi, M.; Chaston, T.; Mikkonen, A.; Martin, J.; Taylor, M.; et al. Arsenic in Soil: A Critical and Scoping Review of Exposure Pathways and Health Impacts. *Environments* **2025**, *12*, 161. [CrossRef]
68. Han, Z.; Yang, J.; Yan, Y.; Zhao, C.; Wan, X.; Ma, C.; Shi, H. Quantifying the Impact of Factors on Soil Available Arsenic Using Machine Learning. *Environ. Pollut.* **2024**, *359*, 124572. [CrossRef]
69. Mandal, J. Decoding Arsenic Mobility in Soils: Machine Learning Insights into PH-Organic Carbon Interactions Across Global Texture Classes. *Earth Syst. Environ.* **2025**, 1–13. [CrossRef]
70. Hao, Y.; Mao, J.; Bachmann, C.M.; Hoffman, F.M.; Koren, G.; Chen, H.; Tian, H.; Liu, J.; Tao, J.; Tang, J.; et al. Soil Moisture Controls over Carbon Sequestration and Greenhouse Gas Emissions: A Review. *npj Clim. Atmos. Sci.* **2025**, *8*, 16. [CrossRef]
71. Šimanský, V.; Lukac, M. Interactions Between Soil Texture and Cover Crop Diversity Shape Carbon Dynamics and Aggregate Stability. *Land* **2025**, *14*, 2044. [CrossRef]
72. Zhou, M.; Li, Y. Spatial Patterns and Mechanism of the Impact of Soil Salinity on Potentially Toxic Elements in Coastal Areas. *Sci. Total Environ.* **2024**, *951*, 175802. [CrossRef]
73. Yan, Z.; Ding, W.; Xie, G.; Yan, M.; Han, Y.; Xiong, X. Quantitative Relationship between Soil PH and Electrical Conductivity Values and Cadmium Phytoavailability for Chinese Cabbage under Simulated Conditions. *Ecotoxicol. Environ. Saf.* **2023**, *266*, 115566. [CrossRef] [PubMed]
74. Zhao, S.; Feng, C.; Wang, D.; Liu, Y.; Shen, Z. Salinity Increases the Mobility of Cd, Cu, Mn, and Pb in the Sediments of Yangtze Estuary: Relative Role of Sediments' Properties and Metal Speciation. *Chemosphere* **2013**, *91*, 977–984. [CrossRef]
75. Van, H.-T.; Hoang, V.H.; Nga, L.T.Q.; Nguyen, V.Q. Effects of Zn Pollution on Soil: Pollution Sources, Impacts and Solutions. *Results Surf. Interfaces* **2024**, *17*, 100360. [CrossRef]

76. Tang, H.; Deng, Q.; Yuan, Y.; Zhang, S.; Luo, Y.; Chen, Y.; Jiang, L.; Huang, Y. The Spatial Distribution and Source of Heavy Metals in Soil-Plant-Atmosphere System in a Large Coal Mining Area. *Ore Energy Resour. Geol.* **2024**, *17*, 100059. [CrossRef]
77. Kubier, A.; Wilkin, R.T.; Pichler, T. Cadmium in Soils and Groundwater: A Review. *Appl. Geochem.* **2019**, *108*, 104388. [CrossRef]
78. Balabanova, B.; Stafilov, T.; Šajn, R.; Tănăselia, C. Geochemical Hunting of Lithogenic and Anthropogenic Impacts on Polymetallic Distribution (Bregalnica River Basin, Republic of Macedonia). *J. Environ. Sci. Health Part A* **2016**, *51*, 1180–1194. [CrossRef]
79. Zhang, Y.; Jiang, S.; Wang, H.; Yu, L.; Li, C.; Ding, L.; Shao, G. Interactions of Fe, Mn, Zn, and Cd in Soil–Rice Systems: Implications for Reducing Cd Accumulation in Rice. *Toxics* **2025**, *13*, 633. [CrossRef]
80. Wyszkowski, M.; Brodowska, M.S. Content of Trace Elements in Soil Fertilized with Potassium and Nitrogen. *Agriculture* **2020**, *10*, 398. [CrossRef]
81. Bani, A.; Gjeta, E.; Pavlova, D.; Ibro, V.; Shahu, E.; Shallari, S.; Selvi, F.; Hipfinger, C.; Puschenreiter, M.; Echevarria, G. Nickel Accumulation in Plants from the Shebenik Mountain Massif, Albania. *Ecol. Res.* **2024**, *39*, 894–908. [CrossRef]
82. Rinklebe, J.; Shaheen, S.M. Assessing the Mobilization of Cadmium, Lead, and Nickel Using a Seven-Step Sequential Extraction Technique in Contaminated Floodplain Soil Profiles Along the Central Elbe River, Germany. *Water Air Soil Pollut.* **2014**, *225*, 2039. [CrossRef]
83. Ibrahim, K.; Bijaksana, S.; Harlianti, U.; Suryanata, P.B.; Ngkoimani, L.O.; Asfar, S.; Fajar, S.J. Pedogenesis of Lateritic Soils and the Enrichment of Critical Metals: A Study from Southeast Sulawesi, Indonesia. *Rud. Geološko Naft. Zb.* **2023**, *38*, 87–98. [CrossRef]
84. Jeske, A. Mobility and Distribution of Barium and Strontium in Profiles of Podzolic Soils. *Soil Sci. Annu.* **2013**, *64*, 2–7. [CrossRef]
85. Myrvang, M.B.; Bleken, M.A.; Krogstad, T.; Heim, M.; Gjengedal, E. Can Liming Reduce Barium Uptake by Agricultural Plants Grown on Sandy Soil? *J. Plant Nutr. Soil Sci.* **2016**, *179*, 557–565. [CrossRef]
86. Sharma, S.; Bolan, S.; Mukherjee, S.; Guimarães Guilherme, L.R.; Gomes Viana, D.; Duim Ferreira, A.; Bakke Myrvang, M.; Almås, Å.R.; Folven Gjengedal, E.L.; Cappuyns, V.; et al. Barium Distribution, Dynamics and Fate in Terrestrial and Aquatic Environments. *Environ. Res.* **2025**, *287*, 123059. [CrossRef]
87. Jia, R.; Huang, X.; Dang, P.; Chen, Q.; Zhong, S.; Fan, F.; Wang, C.; Song, J.; Chorover, J.; Rensing, C. Fe(III) Reduction Mediates Vanadium Release and Reduction in Vanadium Contaminated Paddy Soil under Different Organic Amendments. *Environ. Int.* **2024**, *193*, 109073. [CrossRef]
88. Deng, P.; Yuan, W.; Wang, J.; Li, L.; Zhou, Y.; Beiyuan, J.; Xu, H.; Jiang, S.; Tan, Z.; Gao, Y.; et al. Enhanced Passivation of Thallium, Vanadium and Arsenic in Contaminated Soils: Critical Role of Fe–Mn-Biochar. *Biochar* **2024**, *6*, 61. [CrossRef]
89. Wnuk, E. Mobility, Bioavailability, and Toxicity of Vanadium Regulated by Physicochemical and Biological Properties of the Soil. *J. Soil Sci. Plant Nutr.* **2023**, *23*, 1386–1396. [CrossRef]
90. Du Laing, G.; Rinklebe, J.; Vandecasteele, B.; Meers, E.; Tack, F.M.G. Trace Metal Behaviour in Estuarine and Riverine Floodplain Soils and Sediments: A Review. *Sci. Total Environ.* **2009**, *407*, 3972–3985. [CrossRef] [PubMed]